KERNFORSCHUNGSANLAGE JÜLICH GmbH
Institut für Festkörperforschung

Electron-Phonon Interaction in Chevrel-Phase Compounds

by

F. Pobell, D. Rainer, H. Wühl

Jül - 1710
März 1981
ISSN 0366-0885

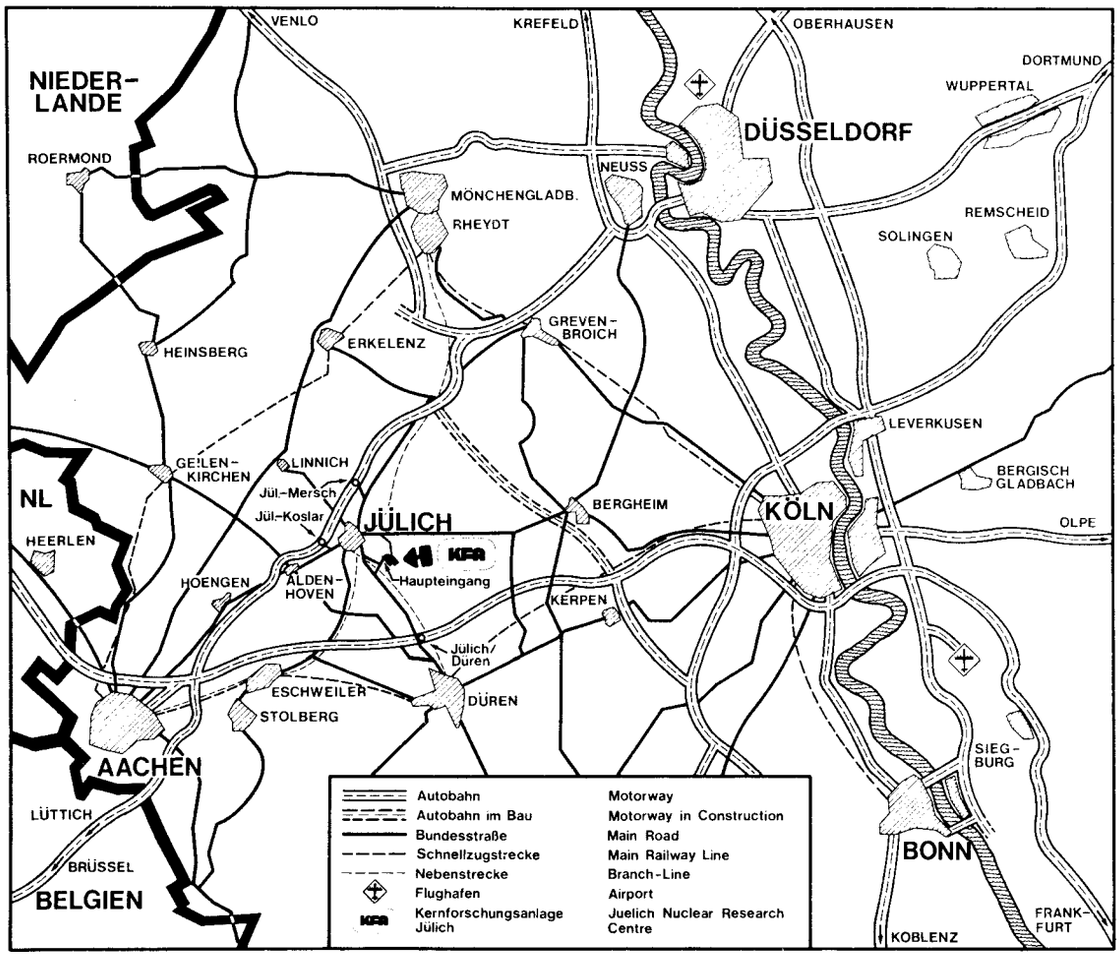

Als Manuskript gedruckt

Berichte der Kernforschungsanlage Jülich - Nr. 1710

Institut für Festkörperforschung Jül - 1710

Zu beziehen durch: ZENTRALBIBLIOTHEK der Kernforschungsanlage Jülich GmbH

Postfach 1913 · D-5170 Jülich 1 (Bundesrepublik Deutschland)

Telefon: (02461) 61-0 · Telex: 833556 kfa d

Electron-Phonon Interaction in Chevrel-Phase Compounds

by

F. Pobell*, D. Rainer** and H. Wühl***

* Institut für Festkörperforschung
Kernforschungsanlage Jülich, D-5170 Jülich, W.-Germany

** Physikalisches Institut der Universität Bayreuth
D-8580 Bayreuth, W.-Germany

*** Kernforschungszentrum Karlsruhe, Institut für Technische Physik
and Universität Karlsruhe
D-7500 Karlsruhe, W.-Germany

Chapter 7 in Volume A of "Superconductivity in Ternary Compounds"
Editors O. Fischer and M. B. Maple
in the Series "Topics in Current Physics"
Springer-Verlag, Berlin, Heidelberg, New York (1981)

Table of contents:

I. Introduction

In this chapter, experiments on the electron-phonon interaction in Chevrel-phase compounds (CPC) and a theoretical discussion of their results will be presented. We will particularly discuss measurements of the isotope effect (1-4) and tunneling spectroscopy experiments (5,6). These investigations have been performed to get information about the strength of the electron-phonon interaction in CPC, and about the question whether there are phonon modes which couple particularly strongly to the electrons in these compounds.

The effect of the electron-phonon interaction on various physical properties of metals such as the heat capacity, transport properties, phonon damping, or superconducting properties is among the most thoroughly theoretically investigated and best understood fields of solid state physics. A recent review and an extensive list of references can be found in Grimvall's article (7) . The main development started when it became clear that an understanding of the superconducting transition temperature needs a quantitatively correct description of electron-phonon effects. Some fortunate circumstances, like the existence of a conveniently

small expansion parameter ($\sqrt{m_{el}/M_{ion}}$), allowed a very accurate theory of the effects of the electron-phonon interaction in metals to be developed, with an estimated error in the range of a few percent. This accuracy has been verified, in particular for superconductors where the theory is known as "strong coupling theory of superconductivity".

Extensive theoretical investigations have shown that most low energy properties of metals are strongly influenced by the electron-phonon interaction, and hence carry information about this interaction. In view of these facts, it is at first sight surprising how little experimental information on the various electron-phonon interaction parameters is available for many of the materials of interest. There is a lack of data even for elements like the transition metals V, Pd, Mo, Ta ..., and almost nothing is known about complicated compounds such as the CPC. This unsatisfactory situation is primarily a consequence of serious difficulties in disentangling effects due to the coupling of conduction electrons to phonons from so-called "band-structure effects". In general, both classes of effects contribute equally to the measured effects. The notion "band-structure effects" in conduction electron properties means a collection of phenomena which are best described by "everything else but electron-phonon effects". This includes effects of the rigid (periodic) background potential as well

as correlation effects caused by the electron-electron interaction.

The important difference between band-structure and electron-phonon effects is their characteristic energy (frequency) scale. The typical energy for band-structure effects is of the order of one Ry, and is set by quantities like the conduction bandwidth, the Fermi energy, the plasmon frequency, or typical spin-fluctuation frequencies. Consequently, one needs frequencies of about 10^{15} Hz or temperatures of the order of 10^5 K in order to "break up" the electron-electron correlations and to see "dynamical band-structure effects". In contrast, electron-phonon effects, i. e., the correlations between conduction electrons and lattice motions start breaking up at frequencies of order ω_D ($\simeq 10^{13}$ Hz) or at the corresponding temperatures θ_D ($\simeq$400 K). The pronounced separation in energy is a consequence of the large difference in the masses of electrons and nuclei, and is necessary for a reasonable distinction between band-structure effects and electron-phonon effects. This condition of separation is, indeed, well fulfilled for conventional metals, and is expected to also hold in Chevrel-phase metals. There is no indication of dangerous soft electronic modes in CPC. The typical energy for the conduction band is about 1eV (8,9,10,10a) which is quite small but still much larger than the typical phonon energy.

Like all known superconducting metals, CPC are not on the verge of being itinerant magnets, which excludes soft paramagons. There is also no evidence for soft plasmons in these compounds. Therefore, it is reasonable to assume that they can be described by the conventional theory of electron-phonon coupling and we will make this assumption throughout. The separation in energy of band-structure and electron-phonon effects is of particular importance for measurements of electron-phonon interaction parameters.

Electron-phonon induced features in conduction electron properties are most pronounced in the superconducting state. Hence, the most valuable information is usually obtained from measurements of superconducting properties. In fact, our present - admittedly rather limited - knowledge of electron-phonon interaction parameters in CPC comes nearly entirely from measurements in their superconducting state. These experiments and their analysis will be discussed in detail in later sections. To our knowledge, the only normal-state data in CPC which have been analyzed with regard to electron-phonon parameters

are the temperature dependence of the normal state resistivity and the electronic specific heat coefficient. We refer to their results in section II.

Before going into the details of experiments on the electron-phonon coupling we will mention some of the properties of CPC which will be needed later for an understanding of the results of these experiments.

The general formula of ternary CPC is $A_vMo_6X_8$, where A stands for a large number of metals (or can be absent), X = S, Se or Te, and v = 0 to 4. Many of the remarkable properties of CPC are intimately related to their unique (mostly hexagonal rhombohedral) crystal structure (12,13). The main building blocks are the almost-cubic units Mo_6X_8. They - and especially their Mo_6 octahedron - are believed to be essential for many properties of CPC. In the channels between the Mo_6X_8 units, metals A can be inserted. They occupy the origin of the rhombohedral unit cell, or - if A is a small ion - some of 12 sites which are closely grouped around it (13) . This crystal structure is the origin of the remarkable electronic and vibrational properties of CPC.

The influence of the electron-phonon coupling in CPC may have been indicated already by the mode softening observed

in neutron scattering (14-18) and Mößbauer effect (19,20) experiments, as well as by lattice instabilities (21-23) . In addition, at least in some CPC, the structure leads to an anharmonic, large vibrational amplitude of the A atom (22) . The latter is quite considerable in $SnMo_6S_8$, for example, as shown by Mössbauer-effect measurements (19,20) and x-ray structural analysis (24) ; a harmonic model is inadequate for a description in this case.

The unique structure of CPC and the results of heat capacity measurements lead Bader et al. (14,15,25) to introduce a "molecular crystal model" for discussions of the complex lattice dynamics of AMo_6X_8. This simplifying model allowed grouping the 45 normal modes of AMo_6X_8 into 36 hard internal modes of the Mo_6X_8 unit ($E > 18$ meV) and 9 soft external modes of AMo_6X_8 ($E < 18$ meV). The latter contain 3 acoustical and 3 optical translational modes of A and Mo_6X_8, and 3 torsional modes of the Mo_6X_8 unit.

This model has been used in qualitative discussions of various experimental information on CPC, like results from specific heat and inelastic neutron scattering experiments (14-18,25), Mößbauer effect (19,20), or isotope effect (1,2) data. But Yvon (13) has pointed out that at most the Mo_6 octahedron and not the entire Mo_6X_8 unit can be considered as a "rigid molecule". Furthermore, the generalized phonon density of states obtained from the neutron experiments indicated a strong

hybridization of the phonon modes (14-18) . The recent lattice dynamical calculations of Bader and Sinha (11) showed in detail a strong mixing of external and internal modes, for example, of torsional and breathing modes of the Mo_6 octahedron. They demonstrated that Mo_6X_8 can not be treated as quasi-rigid.

In connection with the molecular-crystal concept, it was suggested (14,15,25) that the external modes, particularly the torsional modes which involve relative displacements of the Mo_6 octahedra, are important for the electron-phonon interaction in CPC. We will demonstrate that this concept is incompatible with results for the isotope-effect exponents. This conclusion is supported by the tunneling-spectroscopy data and theoretical arguments.

Rather early, Fischer et. al. (26,27) suggested that superconductivity of CPC is due to the Mo-4d electrons which are strongly localized within the Mo_6 octahedron. This is confirmed by recent band-structure calculations (8-10a) . Andersen, Klose and Nohl (8) showed that the Fermi level falls into a doubly degenerate E_g band of Mo-4d electrons derived from the levels of an isolated Mo_6 octahedron. The very small bandwidth results from the weakness of intercluster coupling which is about an order of magnitude weaker than the intracluster coupling (8-10a) . This implies that the electron-phonon interaction is dominated by intracluster coupling of Mo-d states.

Modes of a rigid cluster interact with the E_g states only via the weak intercluster coupling, and should be unimportant.

Before we discuss in detail the isotope effect and tunneling experiment, we will summarize information on the electron-phonon interaction in CPC which has been obtained from other experiments.

II. Experiments on the electron-phonon coupling

Among the normal-state quantities which are influenced by electron-phonon interaction, it is the electronic specific heat, $C_e = \gamma T$, and the temperature dependence of the electrical resistivity, $\rho(T)$, which have been measured and analyzed. Further information on the coupling strength has been obtained from the temperature dependence of C_e in the superconducting state, from the jump ΔC_e of the specific heat at T_c, from T_c itself, and from EPR and NMR measurements. Measurements of the isotope effect and tunneling experiments contain the most detailed information on the electron-phonon coupling and are discussed separately in sections IV and V. A collection of experimental results on the electronic specific heat coefficient γ, on $\Delta C_e / T_c$, and on the reduced energy gap ratio $2\Delta_o/kT_c$ for some CPC of interest is displayed in Tab. 1.

None of the above mentioned experiments allow a direct determination of any of the parameters like λ or η, ($\lambda=\eta/M\langle\omega^2\rangle$), which are commonly used to characterize the strength of the electron-phonon coupling. They provide, at most, a qualitative estimate of trends in the strength of the coupling (conservative minds might even consider this statement as overly optimistic).

In the coefficient γ of the electronic specific heat which is proportional to the quasiparticle density of states at the Fermi level, $N_\gamma(E_F)$, the electron-phonon interaction shows up as a factor $1 + \lambda$ enhancing the band density of states $N_{BS}(E_F)$. Measurements of γ in CPC are very difficult. Strong deviations of the lattice specific heat from Debye behaviour due to the complicated phonon spectrum raise problems when separating the electronic and lattice contributions in the measured heat capacity. The dependence on stoichiometry or amount of impurity phases seems also to contribute to the large scatter in the data. Furthermore, the bare band density of states is not known. Hence, an estimate of λ from γ measurements barely has significance: We take $PbMo_6S_8$ as a typical example: if one extracts $N_{BS}(E_F)$ from susceptibility data, assuming that the measured susceptibility is unenhanced and arises from spin only, the comparison with N_γ gives a value for λ in $PbMo_6S_8$ of about 1.3 (28) . Taking, on the other hand, an exchange interaction of the size obtained for Mo metal into account in estimating $N_{BS}(E_F)$, the unduly high value $\lambda = 2.5$ has been obtained (8).

The most common way of estimating λ is by means of the empirical McMillan formula for T_c. It expresses T_c in terms of λ, the Coulomb parameter μ^*, and an average phonon frequency.

The most serious uncertainty in estimating λ from measured T_c's arises here from considerable uncertainties in choosing the average phonon frequency. The most popular guess, a frequency centered around 12 meV (the range of intercluster vibrations in the molecular crystal model) yields $\lambda = 1.2$ for $PbMo_6S_8$ (28). A list of λ's obtained in this way ("poor man's λ") is given in refs. (28,29). With these λ values, and using the relations $\gamma \sim N_{BS}(E_F)(1+\lambda)$, a strong dependence of λ on the band density of states $N_{BS}(E_F)$ is obtained for CPC (28,29) as plotted in Fig. 1. Some additional discussion on estimates of λ from T_c's from a more theoretical point of view is given in section III.

Measures for the strength of the electron-phonon interaction are the jump of the electronic specific heat at T_c and the reduced gap $2\Delta_o/kT_c$. Measurements on carefully prepared Mo_6Se_8 samples with at most 3 % impurity phases showed $\Delta C_e/\gamma T_c = 2.25$ (30) . This value is substantially larger than the BCS value 1.43. The enhancement is a pronounced strong-coupling effect which indicates a sizeable coupling to low-frequency phonons, and hence, an unusually large λ parameter (see also Section III). In ref. (30) the full temperature dependence of C_{es} was analyzed by a phenomenological equation of Padamsee et al. (31), and a good fit was obtained using a reduced gap of $2\Delta_o/kT_c = 4.2$. This has to be confronted with

the value of 3.5 which was obtained by Alekseevski et al. (32) from an analysis of their specific heat data. - The most direct information on the gap of Mo_6Se_8 comes from tunneling experiments (32a). The authors find a ratio $2\Delta_o/k\ T_c = 4.1 \pm 0.1$ in agreement with the specific heat data of ref.(30). More data for $2\Delta_o/kT_c$ in CPC, including the tunneling data discussed in section V, are given in table 1.

Another source of information on the electron-phonon coupling has been exploited by Bader and Sinha (11) . They calculated the resistivity $\rho(T)$ in order to get insight into the coupling of distinct phonon groups to the electrons. If all phonon modes are weighted equally , a dependence of $\rho(T)$ proportional to T^2 instead of the usual T^3 law is obtained at $T<4OK$. A T^2- law has been observed in sputtered $PbMo_6S_8$ and other CPC (34,35) . The authors (11) showed the importance of high frequency modes for the T^2 behaviour. The omission of modes associated with the displacements of S atoms or the complete cut-off of all modes with $\omega > 18$ meV lead to deviations from the T^2 behaviour. Modes associated with displacements of the Pb atom have no decisive influence on the temperature dependence. But on the other side, for sintered and single crystalline $PbMo_6S_8$ samples believed to

be free of impurity phases a linear T dependence has been observed (30,33,35).

The strength of the electron-phonon coupling has also been investigated with electron paramagnetic resonance (36) and nuclear magnetic resonance (37). The EPR experiments have been performed on Gd diluted in $SnMo_6S_8$ and $PbMo_6S_8$. From the temperature dependence of the impurity-to-conduction electron relaxation rate, a value for $2\Delta_o/kT_c$ of roughly 5 has been extracted. The temperature dependence of the nuclear spin lattice relaxation rate measured in $PbMo_6S_8$ and $PbMo_6Se_8$ by means of NMR was interpreted by the authors as an indication of an energy gap of only 3.5 kT_c "at both sites of Pb and Se".

Summarizing the experimental evidence, one can say that, although no accurate values for λ are yet available, essentially all or at least most experiments indicate a rather strong electron-phonon coupling in CPC, even for the compounds with a relatively low T_c.

III. Theoretical models for the electron-phonon coupling

Presently available experimental data on the electron-phonon interaction in CPC are much too limited to reveal details of the full coupling constant $g(\vec{k}\upsilon,\vec{k}'\upsilon';j)$ for the transition of a conduction electron with "momentum" $\vec{k}^{(*)}$ in band υ into a state with momentum $\vec{k}'^{(*)}$ in band υ' under the emission (absorption) of a phonon of momentum $(\vec{k}-\vec{k}')^{(*)}$ and branch-index j. One does not even know the Eliashberg function $\alpha^2F(\omega)$ which contains information on some average over electron-phonon processes at the Fermi surface:

$$\alpha^2F(\omega) = N(E_F)\sum_{\upsilon,\upsilon',j} \langle |g(\vec{k}\,\upsilon;\vec{k}'\upsilon';j)|^2 \delta(\omega-\omega_j(\vec{k}-\vec{k}'))\rangle_{FS} \quad , \tag{3.1}$$

a function which enters T_c and other superconducting data. A full determination of $\alpha^2F(\omega)$ which usually comes from a computer inversion of tunneling spectra is still unattainable for Chevrel-phase superconductors (see section V). Adding to the present uncertainty is the absence of detailed information on the lattice dynamics $(\omega_j(\vec{q}))$ in these compounds (see chapter VI of this volume).

(*) All momenta are to be understood "modulo reciprocal lattice vectors".

In such a situation, any theoretical assistance for an interpretation of physical data should pursue the following strategy:

1) one needs plausible models as working hypotheses whereever direct information is missing (models for the lattice dynamics, for the electron-phonon coupling, etc.)

2) from these models one must calculate observable quantities (e.g., the transition temperature, the electric conductivity, etc.)

3) one must judge whether the results are compatible with experimental findings and whether to keep or discard the underlying models.

Starting from a model for the lattice dynamics and for the electron-phonon coupling, one can calculate superconducting properties such as T_c, the isotope effects, the thermodynamic critical field or other thermodynamic quantities, and the tunneling spectrum $\alpha^2F(\omega)$ including the energy gap. A powerful theory, the strong-coupling theory of superconductivity (38), and efficient numerical methods allow a rather easy, fast, and accurate evaluation. Further quantities which are influenced

by the electron-phonon coupling, and which can be calculated for given models, are the temperature dependent resistivity, infrared properties, the Landau damping of phonons, the de Haas-van Alphen effect, the upper critical field (H_{c2}), and others. However, all the latter quantities rely heavily on band-structure models for the electronic quasiparticles at the Fermi surface. This adds further uncertainties and might rule out an adequate check of a particular model of the electron-phonon coupling.

The most widely used model for the Eliashberg function $\alpha^2F(\omega)$ is due to McMillan (39) . It was designed for general superconductors, and has a remarkably small number of parameters. McMillan assumed that the superconducting parameters are insensitive to the details in the shape of $\alpha^2F(\omega)$. For all superconductors a standard shape for $\alpha^2F(\omega)$ is used, namely the phonon density of states of Nb with the low-frequency part cut off. The only adjustable parameters in this model are the scale of the phonon frequencies (it is conventionally fixed by adjusting the maximum frequency in $\alpha^2F(\omega)$ to the maximum phonon frequency), the coupling strength (conventially expressed in terms of λ), and the Coulomb pseudo-potential μ^*. The Eliashberg equations plus the Nb-type shape for $\alpha^2F(\omega)$ (the McMillan model) allows a straightforward computer analysis of important data such as the transition temperature, the excitation gap, the heat

capacity or the thermodynamic critical field. Its most widespread use is to estimate the coupling parameter λ from measurements of T_c, and we have performed such an analysis (40) for several Chevrel phase superconductors. The results are shown in figures 2 and 3, where we display λ versus μ_5^* (the index 5 indicates a high frequency cut-off at five times the maximum phonon frequency). For comparison we have included results from an alternative but a priori no better justified guess for the shape of $\alpha^2F(\omega)$. For each compound we have taken the form of its "generalized phonon density of states" ($G(\omega)$) of ref. (16-18) as model for the corresponding $\alpha^2F(\omega)$ spectrum. The $G(\omega)$ spectra have more spectral weight at low frequencies than the Nb-type spectrum (see figure 4) and this leads to a higher λ value at given T_c and μ_5^*. The substantial differences indicate the sensitivity of T_c to the particular shape of $\alpha^2F(\omega)$ and demonstrate the uncertainties in the determination of λ from T_c measurements alone. Nevertheless, the results displayed in figures 2 and 3 allow an estimate of the λ parameters which should be reasonable, unless the true (and presently unknown) $\alpha^2F(\omega)$ spectra differ significantly from the model spectra.

In addition, we have calculated (40) the zero-temperature energy gap and the heat-capacity jump at T_c for two representative materials (Mo_6Se_8, $PbMo_6S_8$). The results are presented in

Table 2. A comparison with the experimental results of refs. (5,30,32a) (see Table 1 and Sect. II) indicates the importance of the low-frequency part of $\alpha^2F(\omega)$ for CPC. There is no sizeable spectral weight at low frequencies in the Nb-type spectra, whereas the $G(\omega)$-type spectrum has considerable low-frequency contributions. As a consequence, the $G(\omega)$ models yield more pronounced strong-coupling features and better agreement with experiment. But neither the Nb- nor the $G(\omega)$-type spectra yield satisfactory agreement with current experimental data. Although the shape of the $\alpha^2F(\omega)$ spectra could be altered in an arbitrary number of ways to obtain perfect agreement, the benefits would be negligible, since the few known data cannot determine a reasonably unique $\alpha^2F(\omega)$.

It should also be emphasized that the averaging procedure which leads to $\alpha^2F(\omega)$ washes out details of the electron-phonon coupling which are essential for an interpretation of data like the isotope effects in superconducting compounds (41,42). For example, $\alpha^2F(\omega)$ contains only information about the total contribution of the coupling from all atoms. But the additional information on the separate contribution of the coupling to the Mo or to the X atoms is an important ingredient for the explanation of partial isotope effects (see sect. IV). Hence, a more complete analysis of experimental data needs more detailed models for the electron-phonon coupling; two such models have recently been suggested for Chevrel-phase compounds, and will be discussed in the following.

The first approach is based on the "molecular-crystal model" for the lattice dynamics. It has been introduced by Bader et al. (14,15,25) who in addition postulated the dominance of a coupling of conduction electrons to soft external modes of rigid Mo_6X_8 units. This appealingly simple model for the electron-phonon coupling was neither compatible with the observed isotope effect in Mo_6Se_8 (11), see also section IV, nor did its basis, the clear separation of external and internal modes (11), withstand a more detailed lattice dynamical calculation. We shall, therefore, not enter an extensive discussion of this model but refer the interested reader to refs. (1,2,11,14,15,25,41) and to sect. IV.

All present evidence favors an alternative model, the "model of weakly coupled cluster states". In the following we shall discuss this model in more detail. It is a spin-off from band structure calculations by Mattheiss, Fong (9) Andersen, Klose, Nohl (8), and Bullett (10) Even though the approaches of these groups are quite different, they all indicated a very typical and unique feature of the conduction band in Chevrel-phase metals. To a good approximation, the most important states at the Fermi energy originate from the 4 d atomic levels of Mo, and the conduction-electron states can be constructed by first combining the 6X5 atomic levels of a Mo_6 cluster into 30 cluster orbitals. Intracluster

interactions lead to a splitting of the cluster levels of about 10 eV. Cluster orbitals from different cells interact only weakly and form tight-binding bands. The weak intercluster interaction results in narrow bands (about 0.5 eV wide) with a high density of states.

This picture for the conduction band has very definite implications for the electron-phonon coupling. It predicts a much stronger coupling of the conduction electrons to internal deformations of a Mo_6 cluster than to the relative displacement of two neighbouring clusters. The relative size of the couplings to the two distinct types of lattice displacement can be estimated by the ratio of intercluster- to intracluster splitting energies which is of order 0.1. Hence, one may safely neglect intercluster contributions to the electron-phonon coupling, and gain significant simplifications. For example, the high (octahedral) symmetry of an isolated Mo_6 cluster may be utilized fully because the electron-phonon coupling is unaffected by neighbouring cells. Strong selection rules and a small number of electron-phonon coupling parameters result. A conduction band formed from cluster states of E_g type, as has been suggested in Ref. (8) , needs only two coupling parameters (g_1, g_2). They determine the coupling to A_{1g}-type deformations of the Mo_6 octahedron (breathing modes), and to the doubly degenerate E_g-type deformations (cigar modes). Hence, the Hamiltonian for the electron-phonon

interaction has the simple two-parameter form:

$$H_{e\text{-}ph} = \sum_{\sigma i}\sum \Big[g_1 Q_{iA} (C^+_{i1\sigma} C_{i1\sigma} + C^+_{i2\sigma} C_{i2\sigma}) + \\ + g_2 Q_{iE1} (C^+_{i1\sigma} C_{i1\sigma} - C^+_{i2\sigma} C_{i2\sigma}) - \\ - g_2 Q_{iE2} (C^+_{i1\sigma} C_{i2\sigma} + C^+_{i2\sigma} C_{i1\sigma}) \Big] . \qquad (3.2)$$

$C^+_{i1\sigma}$, $C^+_{i2\sigma}$ are creation operators for the two cluster states of E_g symmetry in cell i (Wannier-states), and Q_{iA}, Q_{iE1}, Q_{iE2} are the operators for A_{1g}- and E_g-type deformations of the Mo_6 octahedron in cell i.

This model for the electron-phonon coupling must be joined with the bandstructure model (from which it is derived) and a model for the lattice dynamics in order to allow a complete description of superconducting properties of CPC.
The weakest part of this scheme is the lattice dynamics for which detailed experimental information or reliable models are not yet available. It is therefore still open to future investigations to check whether the model of weakly coupled cluster states provides an adequate description of Chevrel-phase superconductors. The only check presently available is a calculation of the isotope effects (42) which gave reasonable agreement with recent data on Mo_6Se_8 (see also section IV).

It would be encouraging for further theoretical work on CPC if this surprisingly simple model for a complicated system is confirmed by future experiments.

IV. Isotope Effect of T_c in Mo_6Se_8 and $SnMo_6S_8$

1) The Isotope Effect

The mass dependence of T_c is the essential experimental information that electron pairing in superconductors occurs via exchange of phonons (43,44). If the phonon-induced interaction dominates, then the so-called "isotope-effect exponent" β in the equation $T_c M^{\beta} = \text{constant}$ should have a value near 0.5 . For a multicomponent metal, the latter relation has to be generalized to

$$d \log T_c = -\sum_r \beta_r \; d \log M_r \qquad (4.1)$$

$$\text{with} \quad \beta = \sum_r \beta_r \; .$$

The partial isotope effect exponents β_r are the response coefficients of T_c to small changes of the masses M_r of the constituents of the compound. Other than T_c or β, the coefficients β_r can distinguish between contributions from individual constituents.

This was the basic idea behind the experiments on Mo_6Se_8 and $SnMo_6S_8$ (1-4) to be discussed in the following. Of course,

those experiments can also give information on the contribution of particular phonon modes to β_r and T_c if one applies a model to the lattice dynamics of CPC. Therefore the results of these experiments allow - at least partially - answering the question about the influence of the various phonon modes on T_c.

Besides the conventionally considered direct isotope effect, i. e., a mass dependence of the superconducting transition temperature T_c which comes from the mass dependence of the phonons at fixed spring constants, there exist indirect isotope effects. They arise from the mass dependence of the zero-point vibrations of the lattice (45-47). The indirect effects must be subtracted from the experimental results before a comparison to theoretical results for the direct isotope effect is possible.

Usually, these indirect effects are small because they are proportional to some power of the ratio of zero-point displacement to lattice constant). Only in exotic cases, like Pd-H(D) (48), is the isotope effect dominated by indirect mechanisms which in this case is probably due to the strongly anharmonic motion of the H(D) ion (46). For an order of magnitude estimate, we scale the large and inverse indirect exponent of Pd-H(D) with the ratio of the mean square displacements, and find $-0.1 \lesssim \beta^{ind} < 0$ for CPC.

Another indirect effect can result from the mass dependence of the unit cell volume (45). This effect can be expressed as

$$\beta^{ind,V} = - \frac{d \log T_c}{d \log V} \frac{d \log V}{d \log M} \qquad (4.2)$$

It was found to be about + 0.1 for Mo metal which, to our knowledge, is the only case where it has been determined (45).

Using the pressure dependence of T_c and the compressibility κ, the exponent $\beta^{ind,V}$ can be written as

$$\beta^{ind,V} = \frac{1}{\chi T_c} \left(\frac{dT_c}{dp}\right)_o \frac{d \log V}{d \log M} \qquad (4.3)$$

Unfortunately, the value of d log V/d log M is not known for Chevrel-phase superconductors but from the sign of $(dT_c/dp)_o$, (49), we can conclude that $\beta^{ind,V}$ is positive for Mo_6Se_8 and $SnMo_6S_8$. Here, we have assumed the usual negative sign for d log V/d log M of course. As discussed in the next section, it was found that the lattice parameters x of the hexagonal cell of Mo_6Se_8 ($SnMo_6S_8$), which are of order 10 Å, remained constant to 0.005 Å (0.006 Å) at room temperature when the isotopic mass was changed by 8 % (7 %) (2). If we take this value and the values for $(dT_c/dp)_o$ from Ref. 49 and for the compressibility of CPC from Ref. (50), we find $0 < \beta^{ind,V} \lesssim 0.1$ for the isotopic volume exponent for CPC. But let us repeat that the values Δx have been

determined at room temperature, and they are the values for the parameters of the hexagonal cell of CPC and not for a particular constituent, like Sn for example.

We have presented these estimates of indirect isotope effect exponents to confirm our belief that they are of order ±0.1 or smaller in CPC.

2) Sample Preparation

The binary system Mo_6Se_8 is well suited for measurements of partial isotope effect exponents because both atoms have a substantial number of stable isotopes and their mass can independently be varied by about 8 %. For an investigation of the influence of the A atom on T_c, the ternary compound $SnMo_6S_8$ seems to be a good candidate for the same reason. Of course, the expected variation of T_c will only be a few percent. Usually, the transition width of Chevrel-phase superconductors, and the T_c scattering of nominally identical samples are at least a few tenths of a degree. Therefore, the main experimental problem for measuring isotope effects is the synthesis of compounds with a reproducible and sharp transition temperature.

For the experiments of Culetto and Pobell (1-3), the optimal preparation conditions for obtaining single phase samples

with appropriate transitions have been found empirically using natural Mo, Se, S, and Sn as starting materials. Starting compositions $Mo_6Se_{7.6}$ and $Sn_vMo_6S_{7.6}$ were taken (51) , because the stoichiometric composition leads to a $MoSe_2$ contamination (24,52). The preparation procedure allowed simultaneous production of up to 12 samples under identical conditions in one reaction cycle. The resulting samples containing the natural isotope composition have been used to study the T_c scatter of nominally identical substances. In the case of $Mo_6Se_{7.6}$, the maximum T_c scatter was $\Delta T_c = \pm$ 0.015 K, as shown in Fig. 5. The scatter of T_c for samples from different reaction cycles was a few hundredths of a Kelvin for this compound. A careful specific heat study on these samples showed that they contain at most 3% $MoSe_2$ and Mo, (30); x-ray analysis did not indicate any impurity phases to within the resolution of several percent.

In the production of $Sn_vMo_6S_{7.6}$ with v = 0.9 to 1.2, a strong dependence of T_c on v was detected. Absence of impurity phases and the smallest scatter of T_c were observed for samples with the smallest T_c, which occurred for v = 1.2 (2,24). The dependence of T_c on v is the reason for the rather large scatter of up to $\Delta T_c \sim$ 0.14 K for Sn compounds from one reaction cycle, and of $\Delta T_c \sim$ 0.3 K for samples from different reaction cycles. The transition widths were 0.07 K.

For the preparation of the isotope samples (53) , the same procedure was followed. The lattice parameters of the hexagonal cells evaluated from x-ray diffraction diagrams were constant to within ±0.005 Å ($\bar{a}$ = 9.56 Å, $\bar{c}$ = 11.17 Å) for $Mo_6Se_{7.6}$, and to within ±0.006 Å ($\bar{a}$ = 9.16 Å, $\bar{c}$ = 11.34 Å) for $Sn_{1.2}Mo_6S_{7.6}$ (2). All samples were single phase (to within the x-ray detection limit) except for $^{100}Mo_6Se_{7.6}$ which contained a barely detectable amount of an unidentified second phase. The superconducting transitions were measured inductively.

Alekseevskii and Nizhankovskii (4) have also investigated $^{s}Sn^{t}Mo_6S_8$ with s = 112 and 124, and t = 92 and 100, respectively. The main difference in their sample preparation procedure was an additional annealing at 1000°C for up to 100 hours. For $SnMo_6S_8$ samples with natural isotopic composition and prepared in one run, they report a maximum deviation of ± 0.07 K from the mean value of T_c, in agreement with our results (2,3). On the other hand, T_c values for samples from different runs deviated by up to 2 K, from 11.68 K to 13.80 K for $^{124}SnMo_6S_8$, which is substantially larger compared to our deviation of 0.3 K. The transition was measured resistively.

3) Results for the Isotope Effect Exponent

Figure 6 shows the transition curves of the series $Mo_6{}^{m}Se_{7.6}$ and of $^{n}Mo_6Se_{7.6}$, respectively, from Refs. (1-3). A very similar dependence of T_c on isotopic mass is clearly visible in both

cases. Figure 7 shows plots of log T_c versus log M where M is the Mo or Se mass. The experimental data are fitted to the relation T_c = const. $M^{-\beta}$ using a least squares fit procedure (2) . Using the above mentioned value for the T_c scatter of identical samples (ΔT_c = ± 0.015 K) to calculate the standard deviation of ß, the authors obtained for the isotope effect exponents

$$\beta_{Mo} = 0.27 \pm 0.04,$$

$$\beta_{Se} = 0.27 \pm 0.05. \qquad (4.4)$$

Because of the small transition widths, the exponents are independent of the definition of T_c.

In Ref.(4)a value of β_{Mo} = 0.48 ± 0.1 was obtained from T_c measurements on $Sn^{92}Mo_6S_8$ and $Sn^{100}Mo_6S_8$.

Figure 8 shows a plot of log T_c versus log M_{Sn} for $Sn_{1.2}Mo_6S_{7.6}$ obtained from three production cycles (2,3). Because of the larger scatter of T_c, the mean values of T_c of the samples from the three runs have been set equal; Fig. 8 shows therefore only the deviation from this mean value of 11.70 K. The data may suggest an inverse partial isotope effect exponent β_{Sn} of order -0.1. Because of the scatter of the data points, of

the scatter of T_c of nominally identical samples, and because Fig. 8 already includes some statistics (it only shows deviations from the mean value), the authors (2,3) did not claim to have seen a dependence of T_c on the Sn mass; a limit $|\beta_{Sn}| \leq 0.05$ was given (2) .

Alekseevskii and Nizhankovskii (4) have observed a very large negative isotope effect exponent β_{Sn}, which, however, depended on the annealing procedure applied to the samples. For seven series of $^{s}SnMo_6S_8$, each with s = 112 and 124, which were subjected to annealing, a mean value of $\beta_{Sn} = -0.23 \pm 0.04$ was obtained (4) .

4) Discussion of the Measured Isotope Effect

a) Mo_6Se_8

There is the following immediate and basic information available from the data on Mo_6Se_8: first, the result $\beta_{Mo}+\beta_{Se} \sim 0.5$ indicates that the "exotic" properties of CPC do not result from "exotic" interactions; their superconductivity and the electron pairing is dominantly determined by the conventional electron-phonon coupling.

The observation of a total exponent of + 0.54, which means slightly larger than 0.5, might be due to indirect contri-

butions mentioned in sect. IV. 1. With the values $\lambda \simeq 0.8$ (30) and $\mu^* \simeq 0.13$, one would expect a direct total isotope exponent $\beta_{Mo} + \beta_{Se} = 0.45$ (41), and therefore $\beta^{ind} \simeq 0.1$ in agreement with our estimates in sect. IV. 1. In the absence of any further information, we make the plausible assumption that the small indirect contributions are equally distributed between Mo and Se. The second basic information then, the result $\beta_{Mo} \simeq \beta_{Se}$, demonstrates that vibrations of the 6 Mo and the 8 Se atoms contribute about equally to the transition temperature. This is the essential information which we now will use in a more detailed discussion.

A first attempt by the authors of Refs. 1 and 2 to interpret their results was based on the molecular crystal model of Bader et. al.(14,15,25), i. e., on the separation of the 42 phonon modes per unit cell of Mo_6Se_8 into three groups: 3 acoustic translational plus 3 torsional modes of the "rigid" Mo_6Se_8 units (external modes), and 36 internal modes. Each of the three types of modes is characterized by frequencies $\bar{\omega}_{trans}$, $\bar{\omega}_{tors}$, $\bar{\omega}_{int}$, whose mass dependences - which cause the isotope effect - are given by:

$$- d \log \bar{\omega}_i^2 = c_{Mo}^i \, d \log M_{Mo} + c_{Se}^i \, d \log M_{Se} \qquad (4.5)$$

The coefficients c^i_{Mo} and c^i_{Se} describe how much the 6 Mo or the 8 Se atoms contribute to a particular mode. The Se atoms, e. g., contribute much more strongly to torsional modes of a Mo_6Se_8 unit than the Mo atoms. This follows from the picture of torsional modes as rigid librations of Mo_6Se_8 units. A detailed analysis of the molecular crystal model yields c^i_{Se}/c^i_{Mo} values of 1.1, 3.3, and 1.2 for the translational, torsional, and internal modes, respectively (1,2) . For a discussion of the isotope effect the above phonon model must be supplemented by a model for the coupling of conduction electrons to the three groups of phonon modes. An early conjecture (14,15,25) attributed the superconducting properties of CPC to a dominant coupling of conduction electrons to the soft external, particularly to the torsional modes of rigid Mo_6Se_8 units. This could be ruled out by the observed isotope effects. A coupling to torsional modes alone leads to a ratio β_{Se}/β_{Mo} of 3.3, and equal coupling to only translational and torsional modes gives a ratio of 1.6. This must be compared with the experimental result $\beta_{Se}/\beta_{Mo} = 1.0 \pm 0.3$. If one sticks to the molecular crystal model for the lattice dynamics, the only sensible way to explain the partial isotope effects is to assume that the internal modes couple at least as strongly as the external modes to conduction electrons (1,41). This lead the authors of refs. (1,2) to reject the model of "dominant coupling to soft torsional modes" of Refs. (14,15,25). The doubts about the model were supported by subsequent lattice dynamical

calculations of Bader and Sinha (11) which call into question the molecular-crystal model for phonons at all. This removes the basis for the electron-phonon coupling model discussed above and makes a revised interpretation of the isotope effect necessary.

In order to check if the improved phonon model of ref. (11) is compatible with the isotope effects in Mo_6Se_8 one has to add to it a model for the electron-phonon coupling, and to calculate the isotope effect. This has been done by Culetto and Rainer (41,42) , who used the model of "weakly coupled cluster states" described in section III. They evaluated the isotope effect on the basis of standard theory of superconductivity (38) . This amounts to a calculation of the phonon propagator which enters the kernel of the Eliashberg equations, and a subsequent computer solution of the linearized Eliashberg equations. The authors neglected correlations of atomic motions in different cells. This approximation did not influence the calculated isotope effect appreciably, as could be checked by using different embeddings in calculating the lattice modes of a single cell. The agreement of the theoretical results, which are shown in Fig. 9, with experimental data (Eq. 4.4) is good when both the theoretical and experimental uncertainties are taken into account (41,42). This result should not be considered as a proof for the applied models but rather as a check for their consistency with the experiments.
Any other models have to undergo this check of

consistency with the rather stringent requirement of $\beta_{Mo} \simeq \beta_{Se}$.

b) $SnMo_6S_8$

A small direct isotope effect might be expected for the A atom due to the hybridization of its modes with "internal cluster modes" and/or due to the weak overlap of the Mo-d orbitals with the Sn atoms. The small value for β_{Sn} reported in refs. (2) and (3) seems to indicate the minor importance of the Sn modes for superconductivity of $SnMo_6S_8$.

If there is a partial isotope effect of Sn due to indirect effects, then the result of Refs.(2) and (3) is in reasonable agreement with the upper limits calculated in Section IV. 1.

On the other hand, Alekseevskii and Nizhankovskii reported the rather large inverse partial isotope exponent of $\beta_{Sn} = -0.23 \pm 0.04$. (The error seems to be surprisingly small with regard to the scatter of T_c in Ref. (4)). This result fits into an earlier phenomenological observation by Alekseevskii of the dependence of T_c on the mass of the A atom in AMo_6S_8 for A atoms from the same group in the periodic table of the elements (54). The authors of Ref.(4) relate their observation to the strongly anharmonic motion of the Sn atoms in CPC, which has been

indicated by Mößbauer-effect measurements (19,20) and x-ray structure analysis (24), and which is due to the asymmetric compressed S surrounding of the Sn atoms. This would invoke the same origin, a strong anharmonicity, for an inverse indirect isotope effect as in the case of Pd-H(D) (46,48). The limit which has been estimated in Sect. IV. 1 for the isotopic volume effect was calculated with an upper limit for the change of the lattice parameter of the total hexagonal unit cell of $SnMo_6S_8$ due to a mass change at room temperature (2). The behavior of the Sn atom at low temperature may be different. Furthermore, there might be contributions from other indirect effects.

An anomalous indirect tin isotope effect in $SnMo_6S_8$ can therefore not be excluded at present and might fit into the "Chevrel-phase picture" as another of their exotic properties. More experiments have to be performed to solve the question of the partial isotope effect of the A atom in CPC.

V. Tunneling spectroscopy on $Cu_{1.8}Mo_6S_8$ and $PbMo_6S_8$

1) Tunneling experiment

Tunneling spectroscopy offers the only practicable possibility to evaluate the Eliashberg function $\alpha^2F(\omega)$ defined in section III from experimental data. This function contains all information needed for the calculation of thermodynamical properties such as T_c, Δ_o, and H_c of a superconductor. $\alpha^2F(\omega)$ can uniquely reflect the importance of destinct phonon frequencies for superconductivity.

The tunneling density of states which is proportional to the first derivative dI/dV of the current-voltage characteristic of a normal-metal /insulator/ superconductor tunnel junction is used to calculate $\alpha^2F(\omega)$ by inversion of the Eliashberg equations (55). This procedure demands for high-quality junctions which can be obtained for non-transition metals. The properties of the high-T_c superconductors, binary and ternary compounds, are often sensitive to deviations from stoichiometry, impurities and lattice disorder. Surfaces are particularly affected. In addition, most of these compounds form bad, ill-defined tunneling barriers by oxidation. Therefore, the short sampling depth of tunneling electrons resulting from a small Fermi velocity in these compounds with high electronic density of states makes it difficult to probe bulk properties. For $Cu_{1.8}Mo_6S_8$ and $PbMo_6S_8$, Poppe and Wühl (5) succeeded in preparing junctions with suffi-

ciently well defined interfaces. They used bulk samples in order to avoid surface problems of evaporated or sputtered films. The authors could measure quantitatively the gap Δ_0 and observe phonon-induced structures in the tunneling characteristics. The latter results only allow a qualitative analysis and are not yet good enough for a numerical evaluation of $\alpha^2F(\omega)$. Sharp drops in dI/dV or minima in the second derivative d^2I/dV^2 are taken for a rough outline of the behavior of $\alpha^2F(\omega)$.

2) Junction preparation

Starting from bulk materials two methods were used for junction fabrication. $Cu_{1.8}Mo_6S_8$ was probed by means of point contacts. The sample was prepared by reaction of the powdered elements at 1200°C and subsequent melting at 1850°C in a sealed Mo crucible. Clean and smooth surfaces appeared on the polycrystalline sample (T_c = 10.2 K) after pealing off a thin Mo layer. The tunneling contact was made by pressing an oxidized Al tip or an etched Zn-doped GaAs tip onto the sample surface very carefully with a piezoelectric drive. These junctions were very sensitive to mechanical vibrations, especially at high voltages.

Better junction quality was obtained by depositing artifical barriers onto single crystals of $PbMo_6S_8$. The cubic crystals with edge lengths of 0.3 to 0.4 mm were prepared in a solid-state diffusion process. The crystals had T_c's of 11.3 to 12 K and a

transition width of about 0.3 K (6). The tunneling area was masked with GE varnish. Granular Al deposited at 77 K in presence of oxygen and oxidized at room temperature served as tunneling barrier. The junctions were completed with Al films.

3) Results and Discussions

The first derivative dI/dV typical for $Cu_{1.8}Mo_6S_8$ is plotted in Fig. 10. Besides the finite measuring temperature, imperfect tunneling barrier and inhomogeneous pressure distribution at the point contact area contribute to the smearing of the gap structure. Because of the strong pressure dependence of T_c in $Cu_{1.8}Mo_6S_8$ (49), T_c deduced from the vanishing of the energy gap varied from 10.2 to 12.5 K. A rough estimate of contact pressure and the observed increase of T_c with pressure, which is in agreement with data in the literature (49) , proved that the point contact did not impair the superconducting properties. As a measure of junction quality, the ratio of junction impedances (R_s/R_n) measured at zero bias in the superconducting and normal state, respectively, came up to 30. The energy gap Δ_o was taken from the energy of the maximum in dI/dV which had been reduced by 7% to allow for the temperature effect at 1.2 K. The procedure of taking the gap at the energy where $dI/dV=R_n^{-1}$ (55) would yield too small values, as the gap smearing is dominated by other than thermal effects. Gaps between 1.8 and 2.3 meV were obtained. $2\Delta_o/kT_c$, for which the actual T_c at the point contact ($\Delta(T_c) = 0$) was measured in each

experiment, was ranging from 3.9 to 4.2.

The corresponding data for $PbMo_6S_8$ (see Fig. 11) obtained from sandwich junctions typically were $\Delta_o = 2.4$ meV and $2\Delta_o/kT_c = 4.8$. For a few junctions $2\Delta_o/kT_c$ up to 5.5 were observed. Values of up to 4.2 were obtained by taking Δ_o at $dI/dV = R_n^{-1}$. All values for $2\Delta_o/kT_c$ exceed significantly the weak coupling BCS value of 3.5, and indicate the very strong electron-phonon coupling in the investigated CPC. Strong-coupling behavior, $2\Delta_o/kT_c = 4.1$, has also been observed for single crystals of binary Mo_6Se_8, which has been investigated by a vacuum tunneling technique (32a).

Due to the strong coupling, it was possible to observe structures in dI/dV and d^2I/dV^2 corresponding to peaks in $\alpha^2F(\omega)$ for most of the junctions made of $Cu_{1.8}Mo_6S_8$ or $PbMo_6S_8$, in spite of the small sampling depth of tunneling electrons in CPC. But instabilities in the tunneling barriers often gave rise to excessive noise especially at high energies and then prevented the analysis of the data. Structures at energies $\omega \lesssim 20$ meV could be reproduced for more than 30 junctions, whereas at $\omega \gtrsim 20$ meV phonon-induced structures could only be established for 4 sandwich junctions with $PbMo_6S_8$.

The best information on $\alpha^2F(\omega)$ at $\omega < 20$ meV were obtained for $Cu_{1.8}Mo_6S_8$ using point contacts with oxidized Al tips. In Fig. 12 a four traces of d^2I/dV^2 from different samples demonstrate the reproducibility. The magnitude of the dips in

d^2I/dV^2 varies depending on the quality of the junctions. The bars mark the variation of the energetic position of the minima obtained from 20 junctions. The influence of the contact pressure on phonon frequencies is expected to be of minor importance. For comparison, the low-energy part of the generalized phonon density of states $G(\omega)$ obtained by neutron scattering experiments at 5 K (18) are shown in Fig. 12 b. At most energies where characteristic phonons appear in $G(\omega)$ minima in d^2I/dV^2 were observed. Qualitative agreement between both results exists at energies of about 4.5, 6.5, 12.5, and 15 meV. The phonon peak at 12.5 meV is reflected as a well pronounced minimum in only one of the second derivatives shown in Fig. 12a, but it has been observed in 4 other not shown experiments. The existence of a phonon peak at 3 meV could not be confirmed, since elastic neutron scattering dominates at such low energies. Disagreement exists at 8.5 and 10.5 meV. The very strong Einstein-like phonon peak at 8.5 meV is faced with a very weak structure observed only occasionally in d^2I/dV^2. On the other hand, the structure in d^2I/dV^2 at 10.5 meV has no counterpart in $G(\omega)$.

$Cu_{1.8}Mo_6S_8$ transforms at 269 K into a triclinic low-temperature modification in which the Cu atoms condense into pairs (13). The pronounced Einstein-like peak which appears at low temperatures in $G(\omega)$ at 8.5 meV can be attributed to at least one of the optical modes associated with Cu-atom displacements. The absence of comparably strong structure in d^2I/dV^2 at 8.5 meV indicates weak coupling to this mode. The results however, also imply that there is a special mode at 10.5 meV which is not distinguished in $G(\omega)$, but contributes to $\alpha^2F(\omega)$.

Measurements at high energies were considerably improved using $PbMo_6S_8/AlO_x/Al$ sandwich junctions. The differential conductances of a junction measured in the superconducting and normal state are shown in Fig. 13. The strong suppression of the conductance in the superconducting state below that of the normal state at $\omega > 6$ meV implies coupling to a broad band of phonons. Peaks in $\alpha^2F(\omega)$ expected from these results are marked by arrows. Maxima in $G(\omega)$ are indicated on the abscissa. The agreement in the energy positions is fairly good.

The structure in dI/dV of $PbMo_6S_8$ junctions at high energies amounts to about 1% of the junction conductance. Since the height of a step is caused by a peak in $\alpha^2F(\omega)$ weighted with ω^{-2} (38), the pronounced steps at $\omega > 20$ meV indicate a very strong coupling to phonons with high energies.

In the energy range of vibrations attributed to the displacement of the Pb atom ($\omega \simeq 4$ meV), it is conspicious that the peak in $\alpha^2F(\omega)$ lies 0.5 to 1 meV below that of $G(\omega)$. This discrepancy may also hint to a different coupling of modes as in the case of $Cu_{1.8}Mo_6S_8$. For a quantitative analysis one has to mind that the samples used in the neutron scattering (18) and tunneling experiment (5,6) had different composition.

Band-structure calculations (8-10) have shown that superconductivity is primarily associated with the d electrons of the Mo_6 octahedea and the electron-phonon interaction should then be mainly determined by coupling of internal modes of the Mo_6 octahedra to the Mo-d electrons. Displacements of the A atoms as well as of the Mo_6X_8 units may therefore contribute to superconductivity only to the extend as these modes are hybridized with internal modes of the Mo_6 octahedra. But the energies where hybridization takes place do in general not coincide with those of Brillouin-zone boundary modes. Phonons with a relatively small density of states may experience a high electron-phonon coupling leading to an enhanced peak in $\alpha^2F(\omega)$. This effect has possibly been observed at 10.5 meV in $Cu_{1.8}Mo_6S_8$.

Tunneling experiments indicated a weak coupling of conduction electrons to optical modes of A atoms. This implies that the A atoms influence superconductivity mainly in an indirect way by charge transfer to the Mo_6X_8 units which reduces the distortion of the Mo_6 octahedra and alters the electron density

of states at the Fermi level (13). A comparison of the properties of ternary compounds with those of the binary Mo_6Se_8 shows that the optical modes of the A atoms indeed may not be crucial for the electron-phonon coupling strength. They are absent in Mo_6Se_8 but, nevertheless, Mo_6Se_8 shows a high value of $2\Delta_o/kT_c$ (see section II) and pronounced strong coupling effects. It seems that another set of low-frequency modes is responsible for strong-coupling features in binary as well as in ternary CPC.

Conclusion

In the preceding sections, we have summarized our present knowledge about the electron-phonon interaction in Chevrel-phase superconductors. Even though some, partially controversial, information is available, the field is still in its infancy: Tunneling spectroscopy, in general the most informative probe, is not accurate enough to give any quantitative results, except for the size of the energy gap. Conclusive isotope-effect data are only available for Mo_6Se_8, and their interpretation is limited by our ignorance of indirect isotope effects. Any theoretical analysis is suffering from a lack of information on the lattice dynamics of CPC. This negative list could be continued. But the situation is not much different for most other groups of superconducting compounds.

Nevertheless, we consider this article as a reasonable basis and encouragement for further research, and we want to summarize its main and probably most reliable results. The energy-gap data from tunneling experiments on Mo_6Se_8, $Cu_{1.8}Mo_6S_8$ and $PbMo_6S_8$ clearly demonstrate the strong electron-phonon coupling in CPC, in agreement with the rather large jump in the specific heat of Mo_6Se_8. These data hint at a special coupling to low-frequency phonons. The calculated values for the energy gap and for the jump of the specific heat at T_c can only be made compatible with experimental results if a

particulary strong coupling to low-frequency modes is assumed. This raises the question about the particular character of these active low-frequency modes. One might think of optical modes of heavy A atoms: This possibility seems to be ruled out by tunneling data - we think also by the isotope-effect results - and by the fact that strong-coupling anomalies are also found in Mo_6Se_8 which has no A atoms. Another suggestion refers to molecular-crystal-type librational modes. This hypothesis cannot explain recent isotope-effect data. The data for Mo_6Se_8 have shown that only a set of phonon modes can be of importance for superconductivity in CPC to which the Mo and the Se atoms contribute about equally (even though the decisive electronic states are probably dominated by Mo electrons). Bandstructure theory claims that the most important conduction electrons in CPC react predominantly to internal deformations of the Mo octahedra which excludes a reasonably strong coupling to librational and other external modes of molecular-type units.

All these requirements put together lead to a rather stringent characterization of the important phonon modes for superconductivity in CPC. The modes should be soft, be coupled strongly to deformations of the Mo octahedra, and should be equally strongly affected by the Mo and Se masses. Do we have such modes (which might be specified as "soft internal modes") in CPC? To date there is no direct proof for their existence. One has even good

reason to doubt the importance of soft modes for CPC superconductivity. Tunneling data indicate that the superconducting electrons couple especially strongly to high-frequency modes. The assumption of a strong coupling to hard internal modes is compatible with the isotope effects and with theoretical ideas based on band-structure calculations, but cannot explain the pronounced strong-coupling effects in the energy gap and the specific heat. Further experimental data or even a confirmation or improvement of present data is needed in order to resolve the striking discrepancies. One might speculate that these discrepancies are intrinsic and indicate a non-conventional type of superconductivity in CPC, e. g., a system of Josephson-coupled "superconducting molecules" as suggested by Revzen and Ron (57). In our opinion, present uncertainties in the experimental data do not yet justify this fascinating but barely motivated alternative. On the contrary, the good and nearly quantitative agreement of CPC superconductivity with the strong-coupling model of superconductors indicates that all remaining puzzles may find their solution within this conventional model.

Acknowledgement: We are very grateful to Dr. F.J. Culetto and Dr. U. Poppe for their substantial contributions to the work summarized in this article and for many helpful discussions.

REFERENCES

1. F.J. Culetto and F. Pobell, Phys. Rev. Lett. 40, 1104 (1978).
2. F.J. Culetto, Ph.D. Thesis JÜL-Report 1587 (1979).
3. F. Pobell in Proc. Int. Conf. on Ternary Superconductors, Lake Geneva, Wisconsin (1980), eds. B.D. Dunlap, F.Y. Fradin, and G.K. Shenoy.
4. N.E. Alekseevskii and V.I. Nizhankovskii, JETP Letters 31, 58 (1980).
5. U. Poppe and H. Wühl, J. de Physique 39, C6-361 (1978), and to be publ. in J. Low Temp. Phys. (1981).
6. U. Poppe, Ph.D. Thesis, JÜL-Report 1635 (1980).
7. G. Grimvall, Physica Scripta 14, 63 (1976).
8. O.K. Andersen, W. Klose, and H. Nohl, Phys. Rev. B17, 1209 (1978).
9. L.F. Mattheis and C.Y. Fong, Phys.Rev. B15, 1760 (1977).
10. D. W. Bullett, Phys.Rev.Lett. 39, 664 (1977).
10a. T. Jarlborg and A.J. Freeman, Phys.Rev.Lett. 44, 178 (1980); A.J. Freeman and T. Jarlborg, in Proc.Int.Conf. on Ternary Superconductors; eds. B.D. Dunlap, F.Y. Fradin, and G.K. Shenoy, Lake Geneva, Wisconsin (1980).
11. S.D. Bader and S.K. Sinha, Phys.Rev. B18, 3082 (1978).
12. M. Marezio, P.D. Dernier, J.P. Remeika, E. Corenzwit, and B.T. Matthias, Mat.Res.Bull. 8, 657 (1973); O. Bars, J. Guillevic, and J. Grandjean, J.Solid State Chem. 6, 48 (1973); R. Chevrel, M. Sergent, and J. Prigent, Mat.Res.Bull. 9, 1487 (1974).
13. K. Yvon in "Current Topics in Materials Science", Vol. II, Chapt.2,p.53;ed. E. Kaldis; North Holland Publ. Comp. 1979.
14. S.D. Bader, S.K. Sinha, and R.N. Shelton in "Superconductivity in d- and f-Band Metals", p. 209, ed. H.D. Douglass, Plenum, New York (1976).

15. S.D. Bader, G.S. Knapp, S.K. Sinha, P. Schweiß, and B. Renker, Phys.Rev.Lett. 37, 344 (1978).

16. B.P. Schweiss, B. Renker, E. Schneider, and W. Reichardt in "Superconductivity of d- and f-Band Metals", p. 189, ed. H.D. Douglass; Plenum, New York (1976); B.P. Schweiß and B. Renker, Progr. Report of the Teilinstitut Nukleare Festkörperphysik, KfK 2357 (1976).

17. B.P. Schweiss, B. Renker, and J.B. Suck, J.de Physique 39, C6-356 (1978).

18. B.P. Schweiss, B. Renker, R. Flükiger, in Proc. Int. Conf. on Ternary Superconductors, Lake Geneva,Wisconsin (1980), eds. B.D. Dunlap, F.Y. Fradin, and G.K. Shenoy.
We thank Drs. B. Renker and B.P. Schweiss for supplying us with their most recent neutron scattering results.

19. C.W. Kimball, L. Weber, G.v.Landuyt, F.Y. Fradin, B.D. Dunlap, and G.K. Shenoy, Phys.Rev.Lett. 36, 412 (1976).

20. J. Bolz, J. Hauck, and F. Pobell, Z. Physik B25, 351 (1976).

21. A.C. Lawson, Mat.Res.Bull 7, 733 (1972); D.C. Johnston and R.N. Shelton, J.Low Temp.Phys. 26, 561 (1977);

22. K. Yvon, Sol. State Comm. 25, 327 (1978).

23. D.C. Johnston, R.N. Shelton, and J.J. Bugaj, Sol.State Comm. 21, 949 (1977); R. Flükiger, A. Junod, R. Baillif, P. Spitzli, A. Treyvaud, A. Paoli, H. Devantay and J. Muller, Sol.State Comm. 23, 699 (1977).

24. R. Chevrel, C. Rossel, and M. Sergent, J.Less Common Metals 72, 31 (1980).

25. S.D. Bader, G.S. Knapp, and A.T. Aldred, Ferroelectrics 17, 321 (1977).

26. Ø. Fischer, Colloques Int. CNRS No. 242, p.79, Grenoble (1974); Proc. 14. Int.Conf.Low Temp.Phys. Vol. V, p.172, ed. M.Krusius and M. Vuorio, Otaniemi (1975).

27. Ø. Fischer, H. Jones, G. Bongi, M. Sergent, and R. Chevrel, J. Phys. C7, L450 (1974); Ø. Fischer, A. Treyvaud, R. Chevrel, and M. Sergent, Sol.State Comm. 17, 721 (1975).

28. Ø. Fischer, Appl. Phys. 16, 1 (1978).

29. F.Y. Fradin, G.S. Knapp, S.D. Bader, G. Cinader, and C.W. Kimball in "Superconductivity in d- and f-Band Metals", p. 297, ed. D. H. Douglass, Plenum (1976).

30. K.P. Nerz, U. Poppe, F. Pobell, M. Weger, and H. Wühl, in "Superconductivity in d- and f-Band Metals", p. 501, ed. H. Suhl, M.B.Maple; Academic Press, 1980; K.P. Nerz, Ph.D. Thesis, JÜL-Spez 30 (1979).

31. H. Padamsee, J.E. Neighbor, and C.A. Shiffman, J. Low Temp. Phys. 12, 387 (1973).

32. N.E. Alekseevskii, G. Wolf, N.M. Dobrovolskii, and C. Hohlfeld, J. Low Temp. Phys. 38, 253 (1980), and J. Low Temp. Phys. 40, 479 (1980).

32a. U. Poppe, H. Schröder, and F. Pobell, to be published (1981).

33. R. Flükiger, R. Baillif and E. Walker, Mat. Res. Bull 13, 743 (1978).

34. K. Kitazawa, T. Matsuura, and S. Tanaka, in Proc. Int. Conf. on Ternary Superconductors, Lake Geneva, Wisconsin (1980), eds. B.D. Dunlap, F.Y. Fradin, and G.K. Shenoy.

35. J.A. Woollam and S.A. Alterovitz, Solid State Commun. 27, 571 (1978), and Phys. Rev. B 19, 749 (1979).

36. R. Odermatt, M. Hardiman, and J. van Meijel, Solid State Commun. 32, 1227 (1979).

37. N. Sano, T. Taniguchi, and K. Asayama, Solid State Commun 33, 419 (1980).

38. D.J. Scalapino in: "Superconductivity", p.449, ed. R.D. Parks (Marcel Dekker, New York, 1969).

39. W.L. McMillan, Phys. Rev. 167, 331 (1968).

40. We have used the same computer program as Jong-Chul Park, J.E. Neighbor and C.A. Shiffman Phys. Lett. 50 A, 9 (1974).

41. F.J. Culetto and D. Rainer, JÜL-Report 1504 (1978).

42. D.Rainer and F.J. Culetto, Phys.Rev. B19, 2540 (1979).

43. H. Fröhlich, Phys.Rev. 79, 845 (1950);

44. J. Bardeen, Phys.Rev. 80, 567 (1950).

45. T. Nakajima, T. Fukamachi, O. Terasaki, and S. Hosoya, J. Low Temp. Phys. 27, 245 (1977).

46. B.N. Ganguly, Z. Physik B22, 127 (1975), and Phys.Rev. B14, 3848 (1976).

47. R.J. Miller and C.B. Satterthwaite, Phys.Rev.Lett. 34, 144 (1975)

48. B. Stritzker and W. Buckel, Z. Physik 257, 1 (1972).

49. R.N. Shelton, A.C. Lawson, and D.C. Johnston, Mat.Res.Bull. 10, 297 (1975); R.N. Shelton, in "Superconductivity in d- and f-Band Metals", p. 137, ed. D.H. Douglass, Plenum Press (1976); for $Sn_{1.2}Mo_6S_8$ we take $(dT_c/dp) \approx 1.10^{-4}$ (K/bar), which corresponds to the sample with a T_c closer to the one of our sample.

50. A.W. Webb and R.N. Shelton, J. Phys. F8, 261 (1978)

51. It was not investigated whether the appropriate formula for the reaction products is $Mo_6Se_{7.6}$ ($Sn_{1.2}Mo_6S_{7.6}$) or $Mo_{6.3}Se_8$

($Sn_{1.3}Mo_{6.3}S_8$), or whether the reaction product deviated from the starting composition. In Ref. 24, indications were found that reaction of $Sn_{1.2}Mo_{6.35}S_8$ to a single crystal results in a stoichiometric compound. In this article we will often use the stoichiometric formula for convenience.

52. M. Sergent, R. Chevrel, C. Rossel, and Ø. Fischer, J. Less Common Metals 58, 179 (1978).

53. The isotopes were obtained from Rohstoff Einfuhr GmbH, Düsseldorf; their mean masses are 76.15, 77.94, 79.91, 81.68 for Se, 92.17, 94.11, 95.92, 97.75, and 99.61 for Mo, and 115.99, 119.18, 121.78, and 123.86 for Sn, respectively.

54. N.E. Alekseevskii, Cryogenics 26, 257 (1980).

55. W.L. McMillan and J.M. Rowell, in "Superconductivity", p. 561 ed. R.D. Parks (Dekker, New York 1969).

56. R.W. McCallum, L.D. Woolf, R.N. Shelton and M.B. Maple, J. de Physique 39, C6-359 (1978).

57. M. Revzen and A. Ron, private communication (1978).

Table Captions

Table 1: Collection of experimental results on the electronic specific heat coefficient, the specific heat jump at T_c, and on the reduced energy gap at zero temperature. In refs. (5,32a) the gap has been determined from tunneling data whereas in refs. (30,32,36,37) a gap is analyzed from thermodynamic, EPR and NMR measurements, respectively.

Table 2: Reduced specific heat jump and reduced zero-temperature energy gap for two representative Chevrel-phase superconductors, as obtained from a strong-coupling calculation using the two model-$\alpha^2 F(\omega)$ spectra shown in Fig. 4, and $\mu_5^* = 0.13$. For a comparison to experimental results see Tab.1.

	Mo_6Se_8	Mo_6S_8	$PbMo_6S_8$	$Cu_{1.8}Mo_6S_8$	$SnMo_6S_8$	References
γ ($\frac{mJ}{mole\ K^2}$)	44	-	105	-	79	(29)
	47	-	-	-	-	(30)
	75	28	125	63	84	(32,54)
	21	-	-	-	-	(56)
$\Delta C_e/T_c$ ($\frac{mJ}{mole\ K^2}$)	70	-	215	-	155	(29)
	107	-	-	-	-	(30)
	93	-	160	-	104	(32,54)
	41	-	-	-	-	(56)
$\frac{2\Delta_o}{kT_c}$	-	-	4.8	4.2	-	(5)
	4.1	-	-	-	-	(32a)
	4.2	-	-	-	-	(30)
	3.5	-	3.9	-	-	(32)
	-	-	5	-	5	(36)
	-	-	3.5	-	-	(37)

Table 1

	$\Delta C_e/\gamma T_c$	$2\Delta_o/kT_c$
Mo_6Se_8 (Nb-type spectrum)	1.51	3.6
Mo_6Se_8 (G(ω)-type spectrum)	1.76	3.8
$PbMo_6S_8$ (Nb-type spectrum)	1.67	3.7
$PbMo_6S_8$ (G(ω)-type spectrum)	2.07	4.1
BCS	1.43	3.5

Table 2

Figure Captions

Fig. 1: Dependence of the "poor man's" electron-phonon coupling constant λ on the bare density of states at the Fermi level for several CPC; from ref. 28.

Fig. 2: Calculated λ values versus Coulomb pseudo-potential μ^*_5 for Mo_6Se_8 and $PbMo_6S_8$ using two kinds of model spectra. The dashed lines are obtained for McMillan's Nb-type spectrum (39) (see Fig. 4), and the solid lines are for the generalized phonon density of states ($G(\omega)$) of refs. (16-18).

Fig. 3: Calculated λ values versus Coulomb pseudo-potential μ^*_5 for several Chevrel phase superconductors. The results are obtained by taking the generalized phonon density of states of refs. (16-18) as a model for $\alpha^2F(\omega)$ in the corresponding compounds.

Fig. 4: Comparison of the Nb-type spectrum (McMillan's spectrum (39)), and the $G(\omega)$-type spectrum for Mo_6Se_8 (16-18). Both models for $\alpha^2F(\omega)$ yield a T_c of 6.3 K (for $\mu^*_5 = 0.13$)

Fig. 5: Scattering of T_c of 12 nominally identical Mo_6Se_8 samples synthesized in one reaction cycle; from ref . 2.

Fig. 6: Inductively measured superconductive transitions of (a) $Mo_6{}^mSe_{7.6}$ and (b) ${}^nMo_6Se_{7.6}$. The nominal isotopic masses are m = 82,80,78,76, and n = 100,98,96,94,92 from left to right; from refs. 1-3.

Fig. 7: Double-logarithmic plot of T_c versus isotopic mass M of Mo and Se, respectively, in Mo_6Se_8. The lines have slopes of -0.27; from refs. 1-3.

Fig. 8: Double-logarithmic plot of T_c versus isotopic mass of Sn in $^{r}SnMo_6S_8$ for r = 116, 119, 122, and 124. The vertical error bar shows the T_c scatter of nominally identical samples from one reaction cycle. Because the scatter for samples from different reaction cycles is about a factor of two larger, the mean T_c values for the three series have been set equal in this plot; from refs. 2,3.

Fig. 9: Theoretical results for the partial isotope exponents in Mo_6Se_8 in the locator model of ref. 42 for various ratios of the electronic coupling constants η_1/η_o. The full and dashed lines represent the results of rigid background, or periodic boundary conditions, respectively. The overall coupling strength is adjusted to yield a T_c=6.3 K; from ref. 42.

Fig. 10: Differential conductance dI/dV versus voltage of a $Cu_{1.8}Mo_6S_8$-Al point contact junction at 1.1 K; from refs. 5,6.

Fig. 11: Differential conductance dI/dV versus voltage of a $PbMo_6S_8/AlO_x(12\text{Å})/Al$ sandwich junction at 1.2 K; from refs. 5,6.

Fig. 12 a: Second derivative d^2I/dV^2 versus voltage measured from the gap edge for four $Cu_{1.8}Mo_6S_8$/Al point-contact junctions at 1.2 K. The bars show the positions of the minima obtained from about 20 junctions; from refs. 5,6.

b: Generalized phonon density of states $G(\omega)$ of $Cu_{1.83}Mo_7S_8$ from inelastic neutron scattering measured at 5 K; from ref. 18.

Fig. 13: Differential conductance dI/dV of a $PbMo_6S_8/AlO_x/Al$ sandwich junction versus voltage measured at 1.5 K ($<T_c$) and 14 K ($>T_c$). The arrows indicate the position of structure in dI/dV and thus in $\alpha^2F(\omega)$. Circles indicate the energies of characteristic maxima in the phonon density of states $G(\omega)$ counted from the gap edge Δ_o ref. 18; from refs. 5,6.

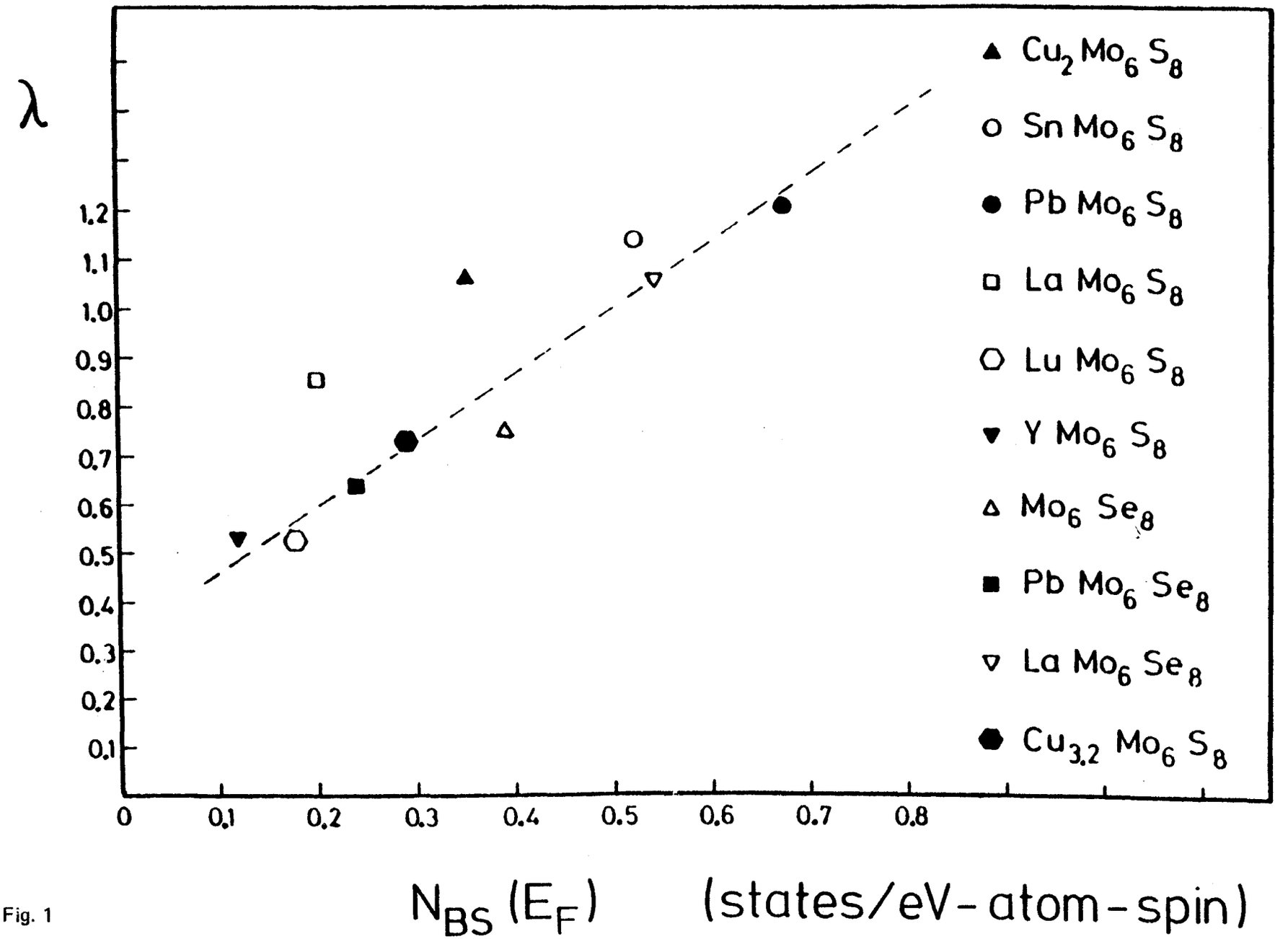
λ
1.2
1.1
1.0
0.9
0.8
0.7
0.6
0.5
0.4
0.3
0.2
0.1
0
0.1
0.2
0.3
0.4
0.5
0.6
0.7
0.8
▲ Cu2 Mo6 S8
○ Sn Mo6 S8
● Pb Mo6 S8
□ La Mo6 S8
○ Lu Mo6 S8
▼ Y Mo6 S8
△ Mo6 Se8
■ Pb Mo6 Se8
▽ La Mo6 Se8
● Cu3.2 Mo6 S8
NBS (EF) (states/eV-atom-spin)

Fig. 1

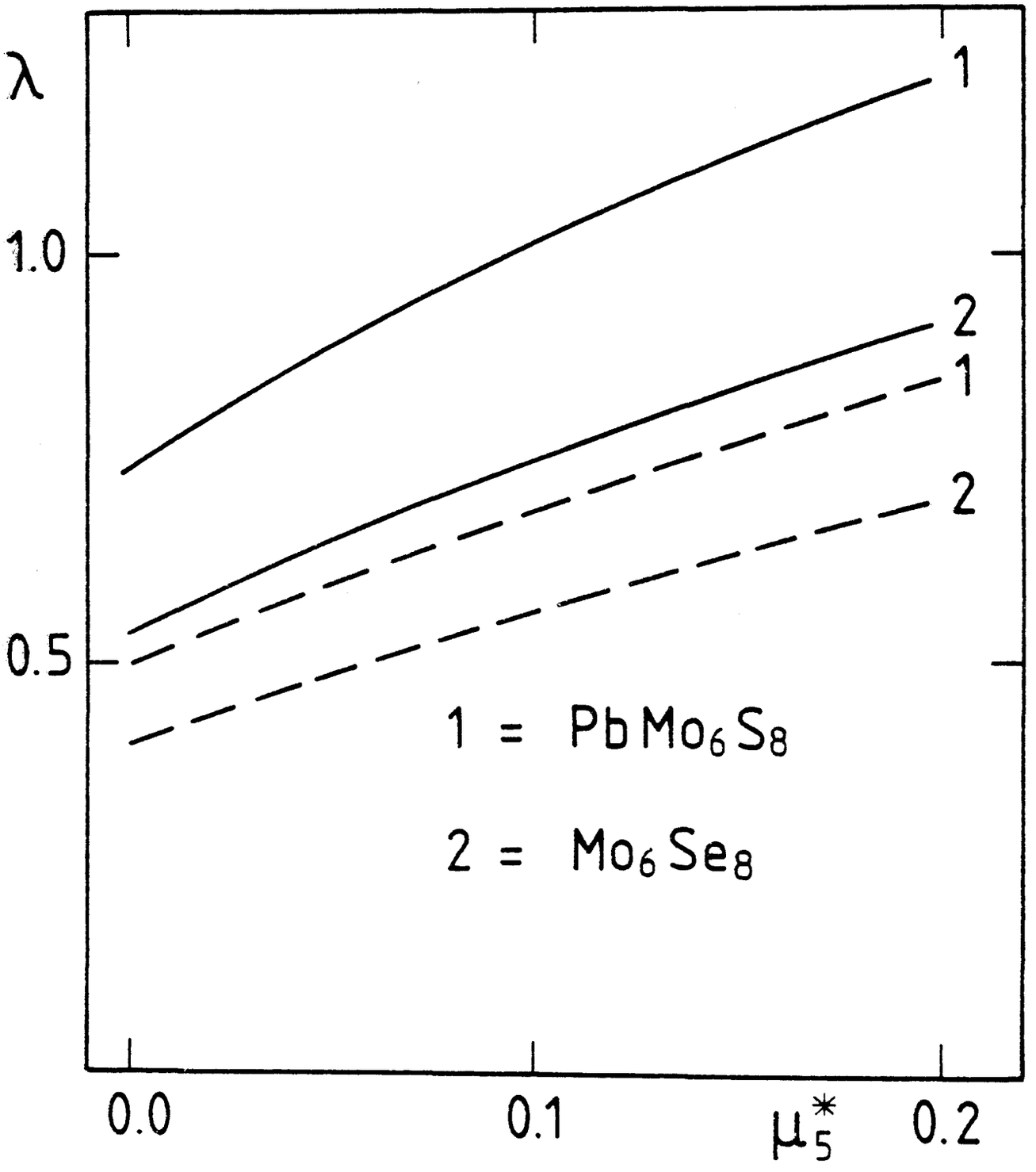

Fig. 2

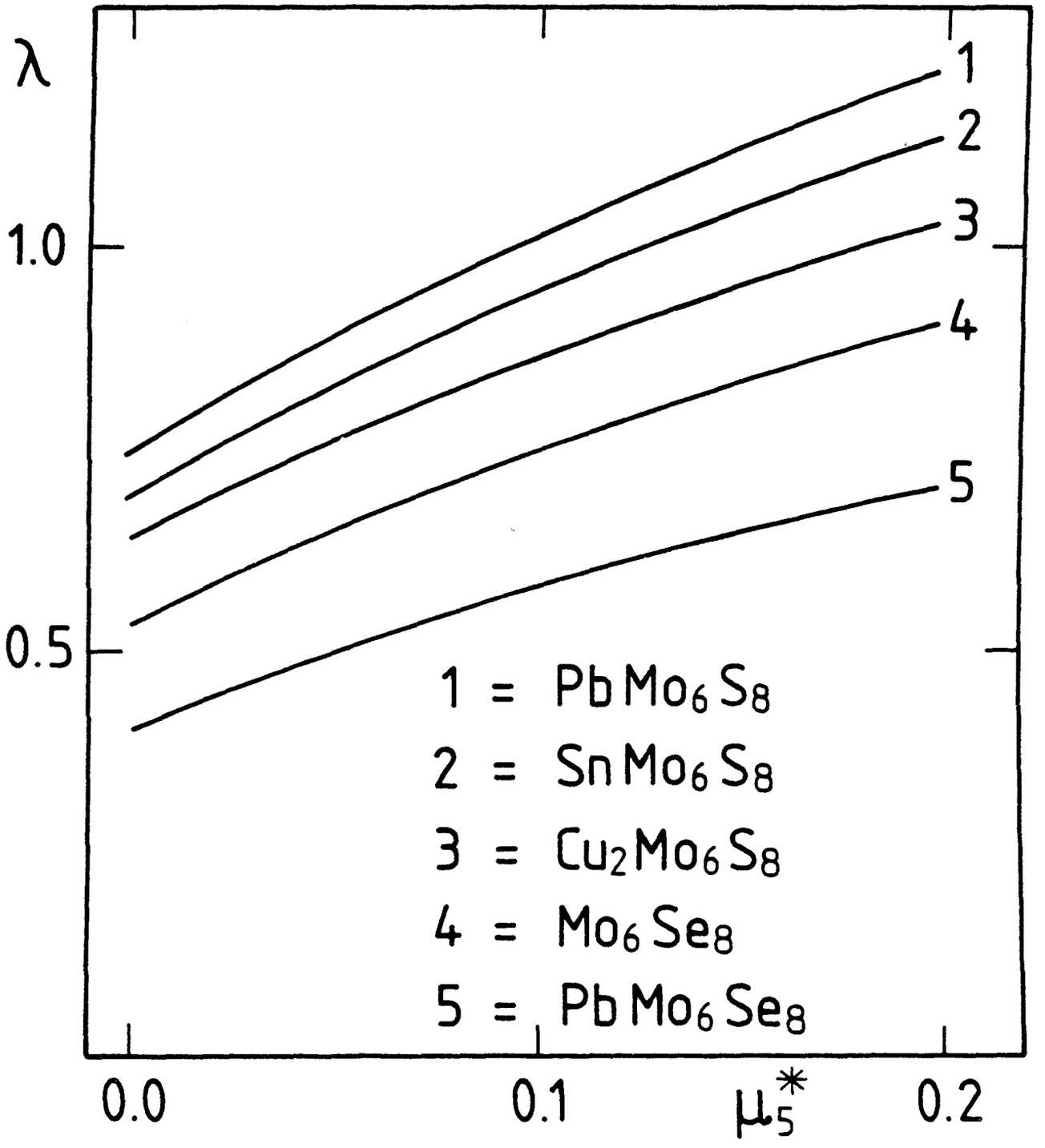
λ
1.0
0.5
1
2
3
4
5
1 = Pb Mo6 S8
2 = Sn Mo6 S8
3 = Cu2 Mo6 S8
4 = Mo6 Se8
5 = Pb Mo6 Se8
0.0
0.1
0.2
μ5*

Fig. 3

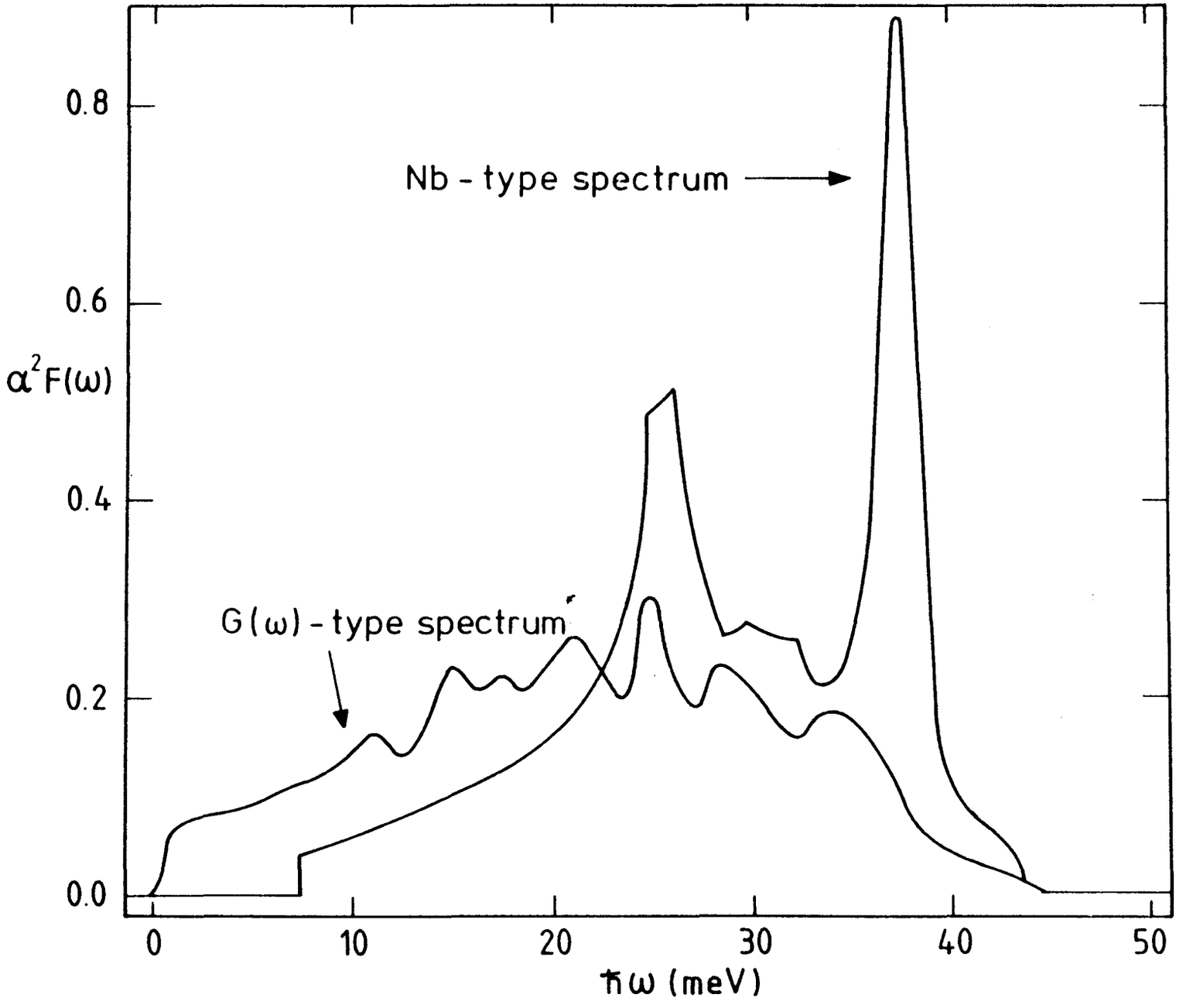
0.8
0.6
0.4
0.2
0.0
$\alpha^2 F(\omega)$
Nb - type spectrum
G(ω) - type spectrum
0
10
20
30
40
50
ħω (meV)

Fig. 4

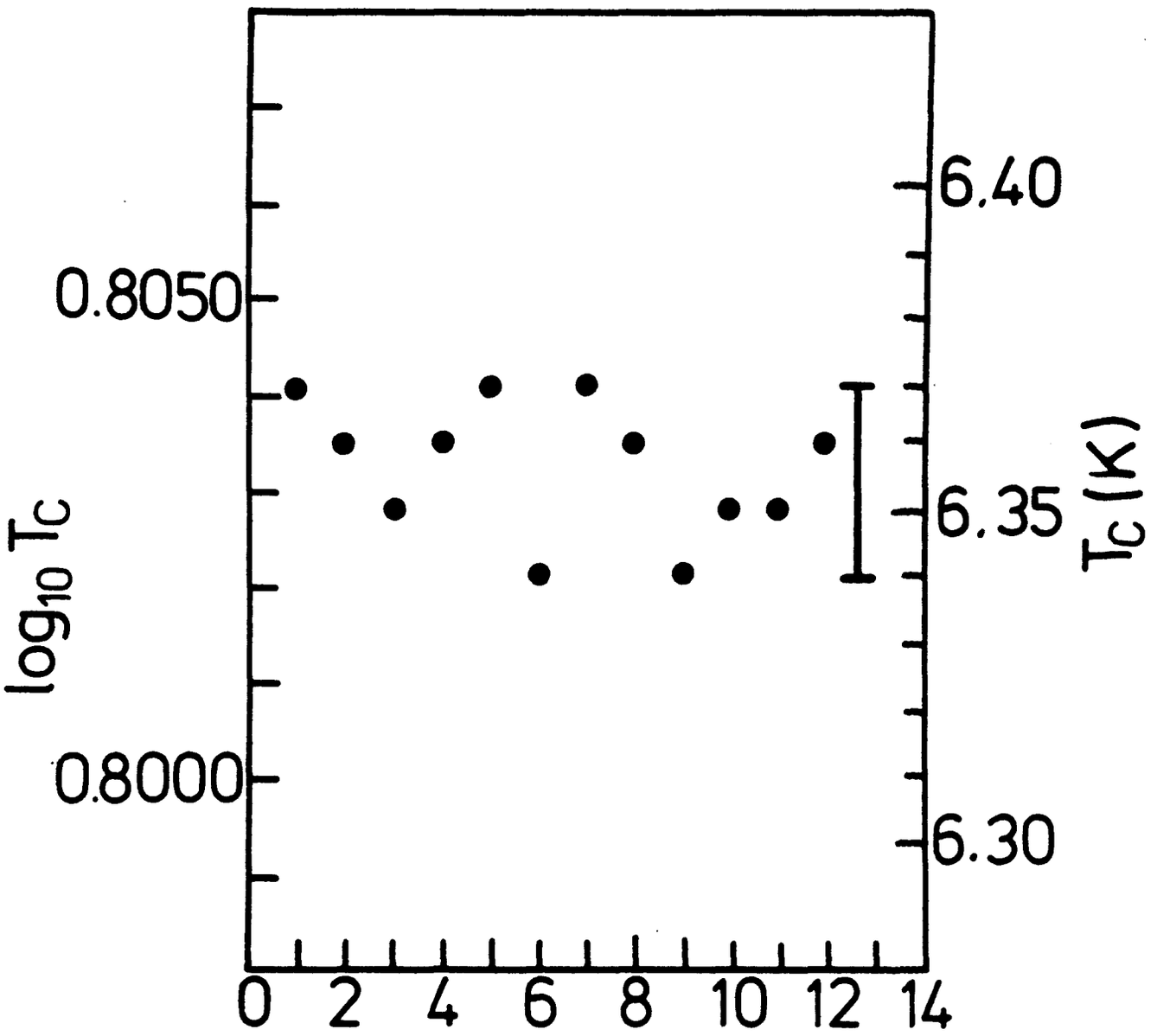

Fig. 5

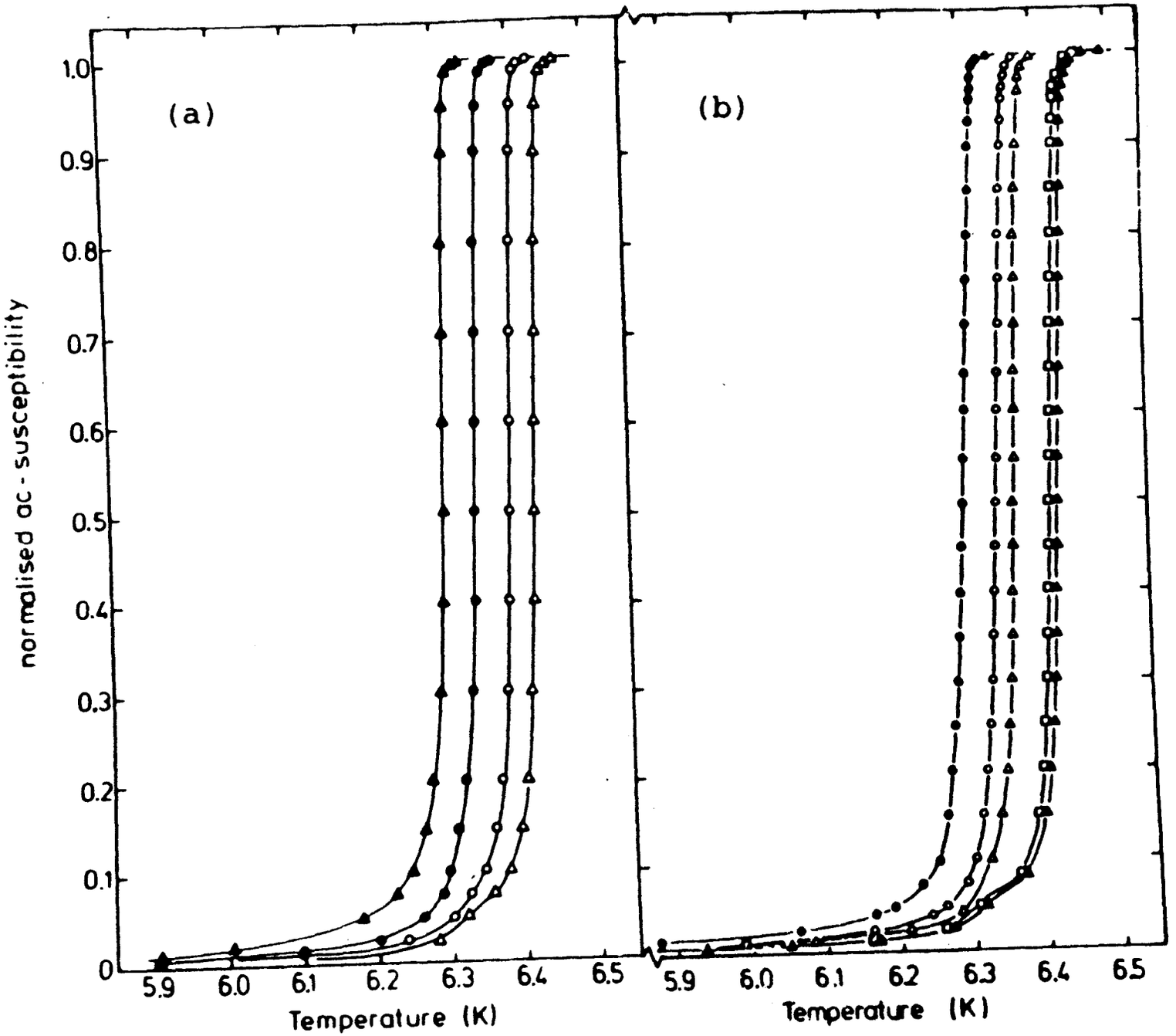
(a)
(b)
normalised ac - susceptibility
1.0
0.9
0.8
0.7
0.6
0.5
0.4
0.3
0.2
0.1
0
5.9
6.0
6.1
6.2
6.3
6.4
6.5
Temperature (K)

Fig. 6

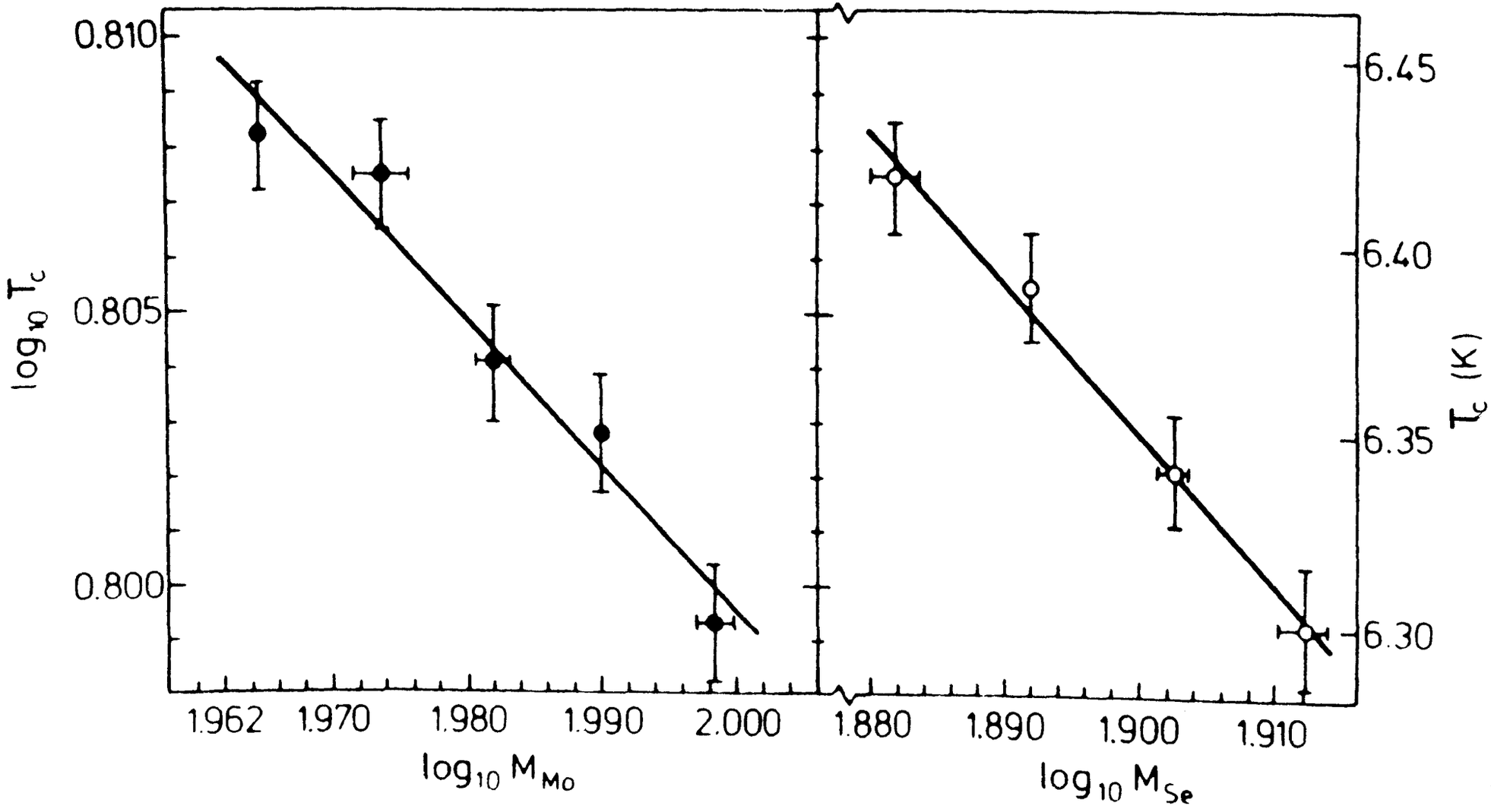
0.810
0.805
0.800
$\log_{10} T_c$
1.962
1.970
1.980
1.990
2.000
$\log_{10} M_{Mo}$
1.880
1.890
1.900
1.910
$\log_{10} M_{Se}$
6.45
6.40
6.35
6.30
T_c (K)

Fig. 7

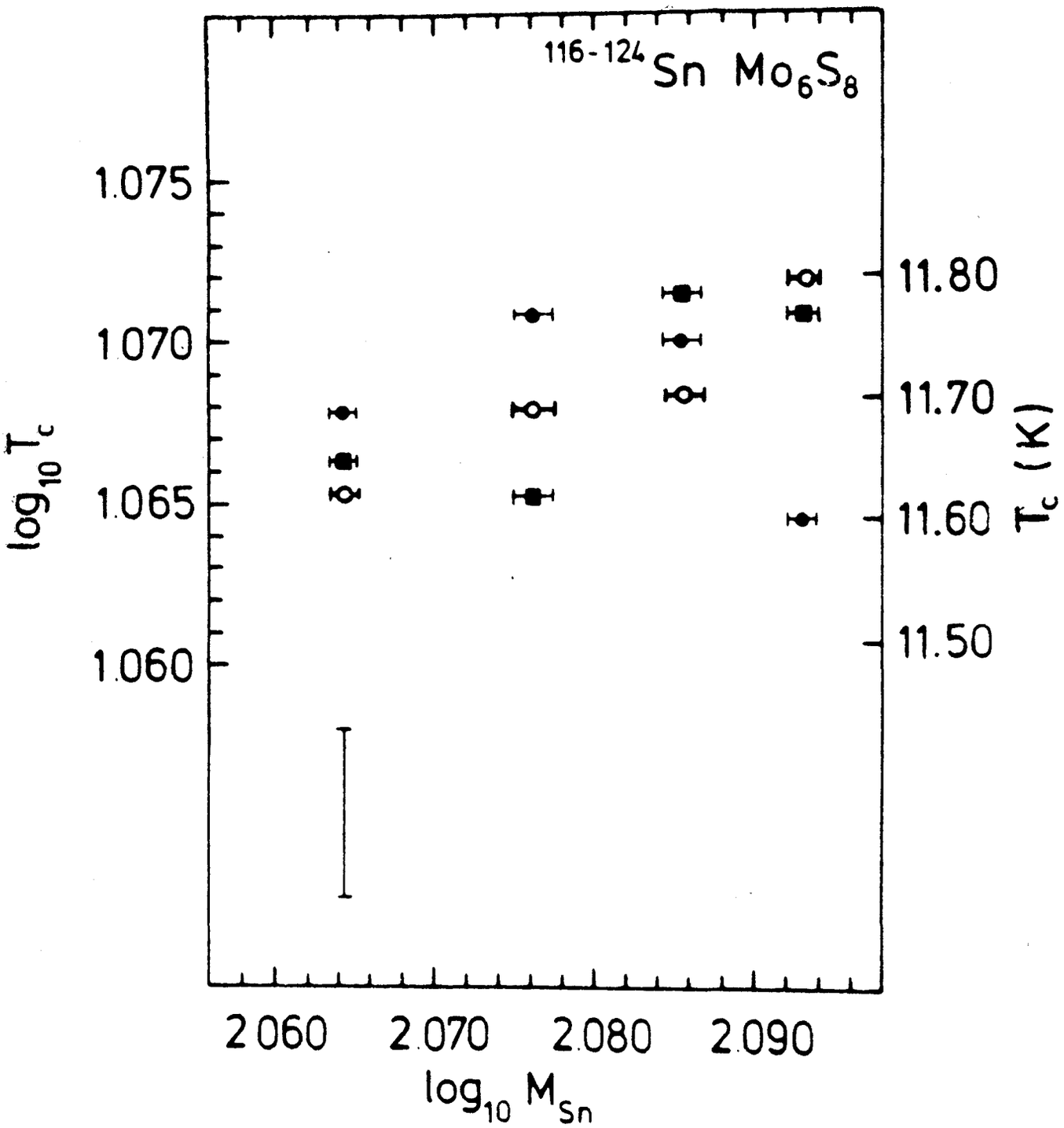
116-124 Sn Mo6S8
1.075
1.070
1.065
1.060
log10 Tc
11.80
11.70
11.60
11.50
Tc (K)
2.060
2.070
2.080
2.090
log10 MSn

Fig. 8

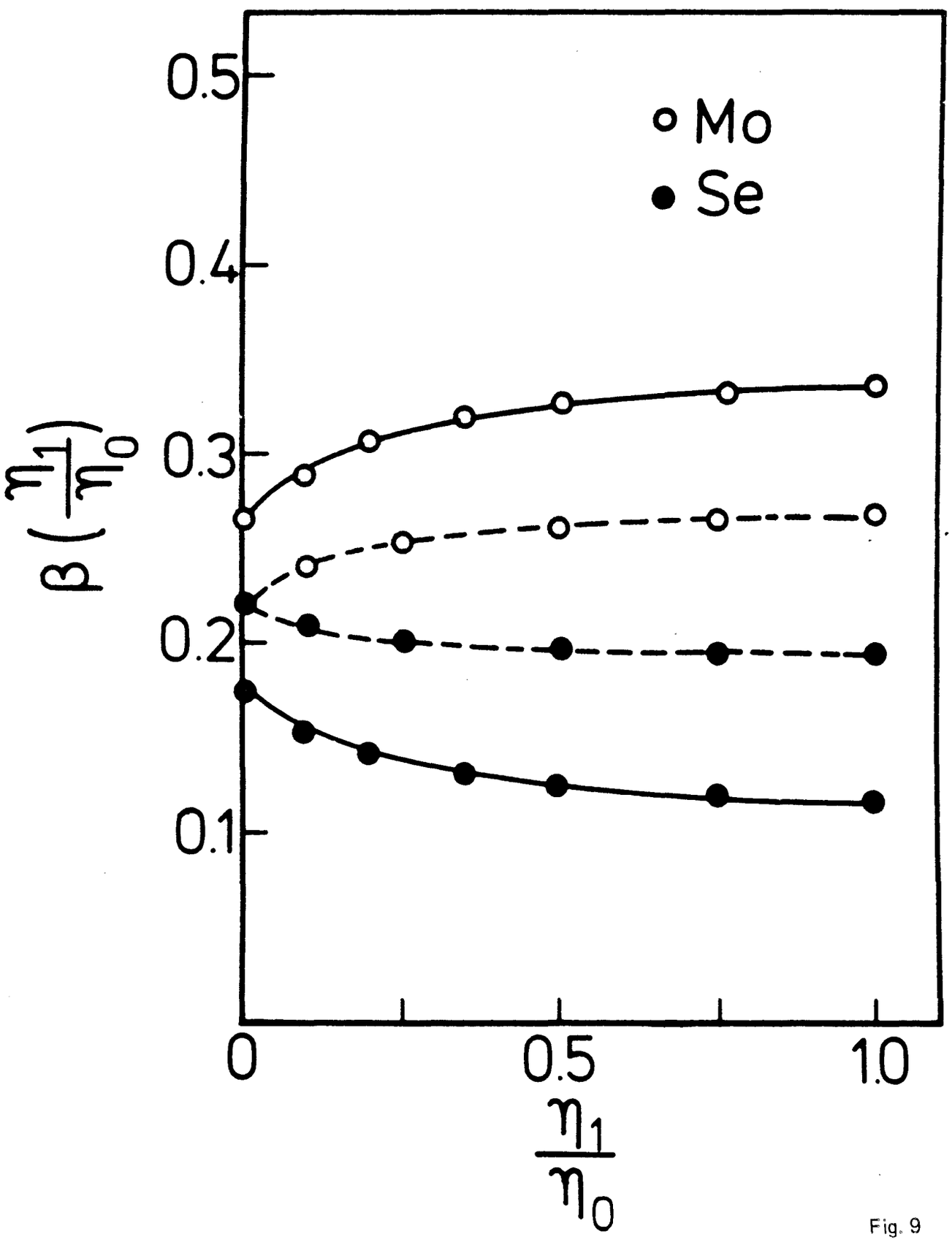
0.5
0.4
0.3
0.2
0.1
0
0.5
1.0
Mo
Se
$\beta\left(\frac{\eta_1}{\eta_0}\right)$
$\frac{\eta_1}{\eta_0}$

Fig. 9

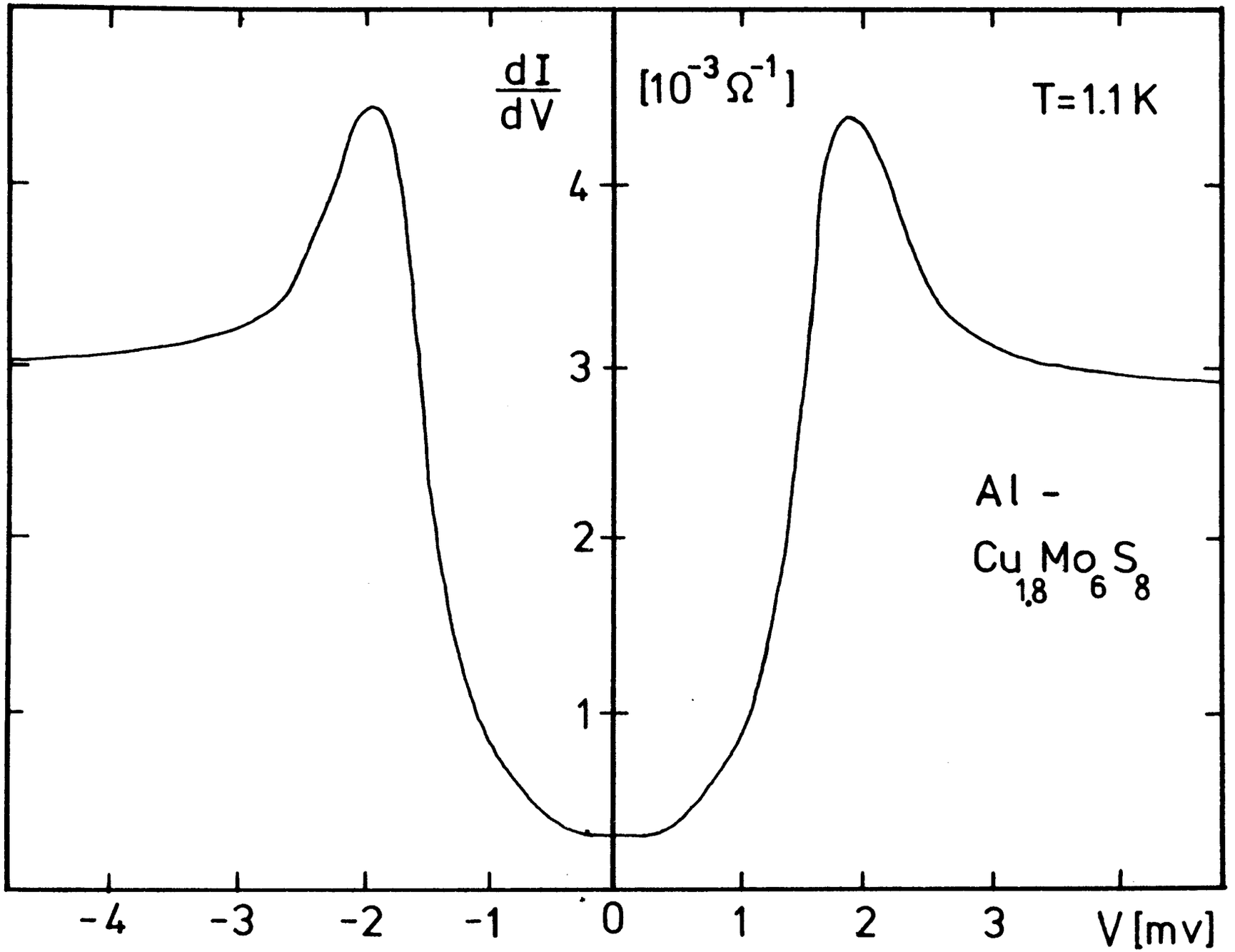

Fig. 10

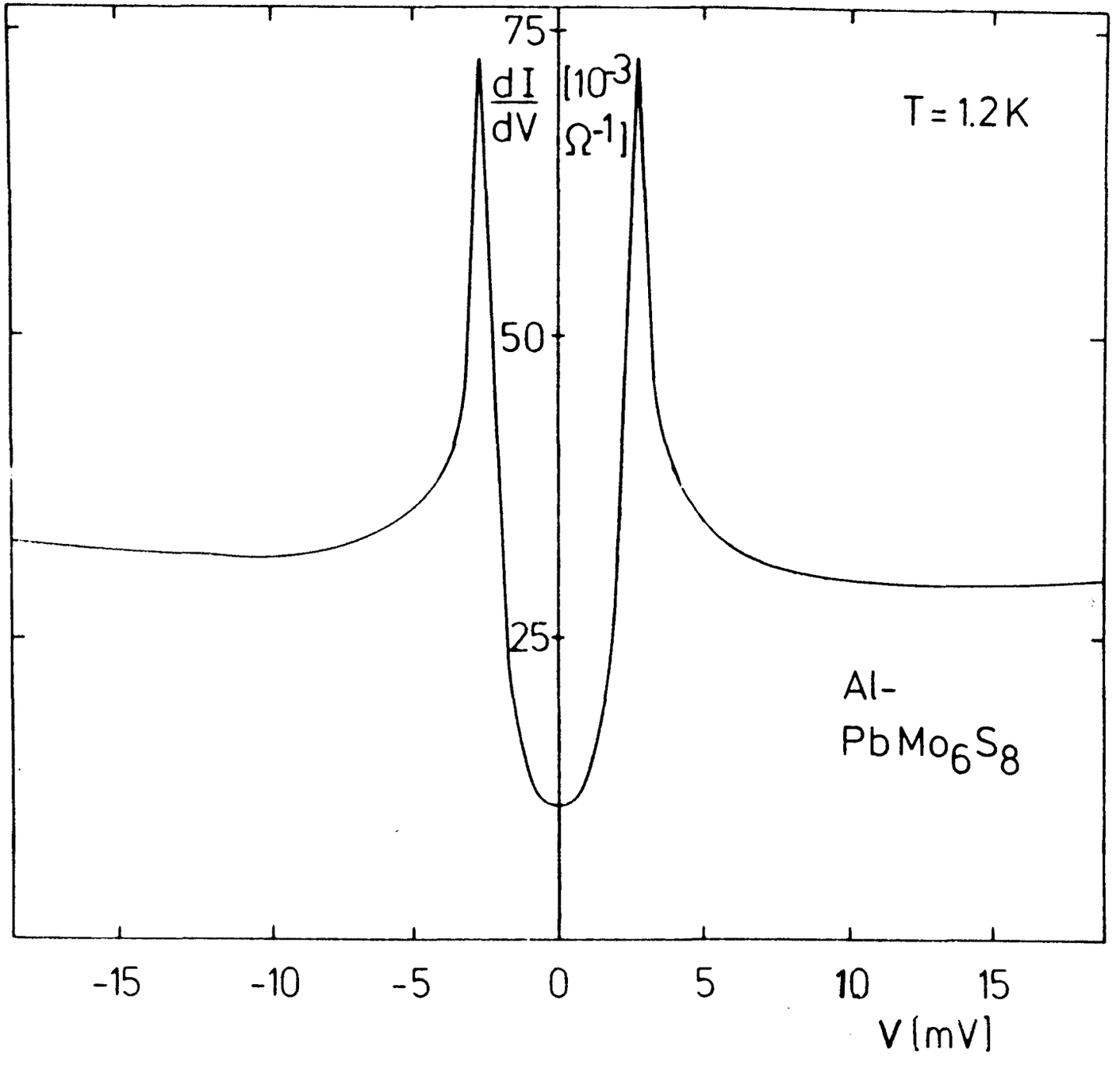

Fig. 11

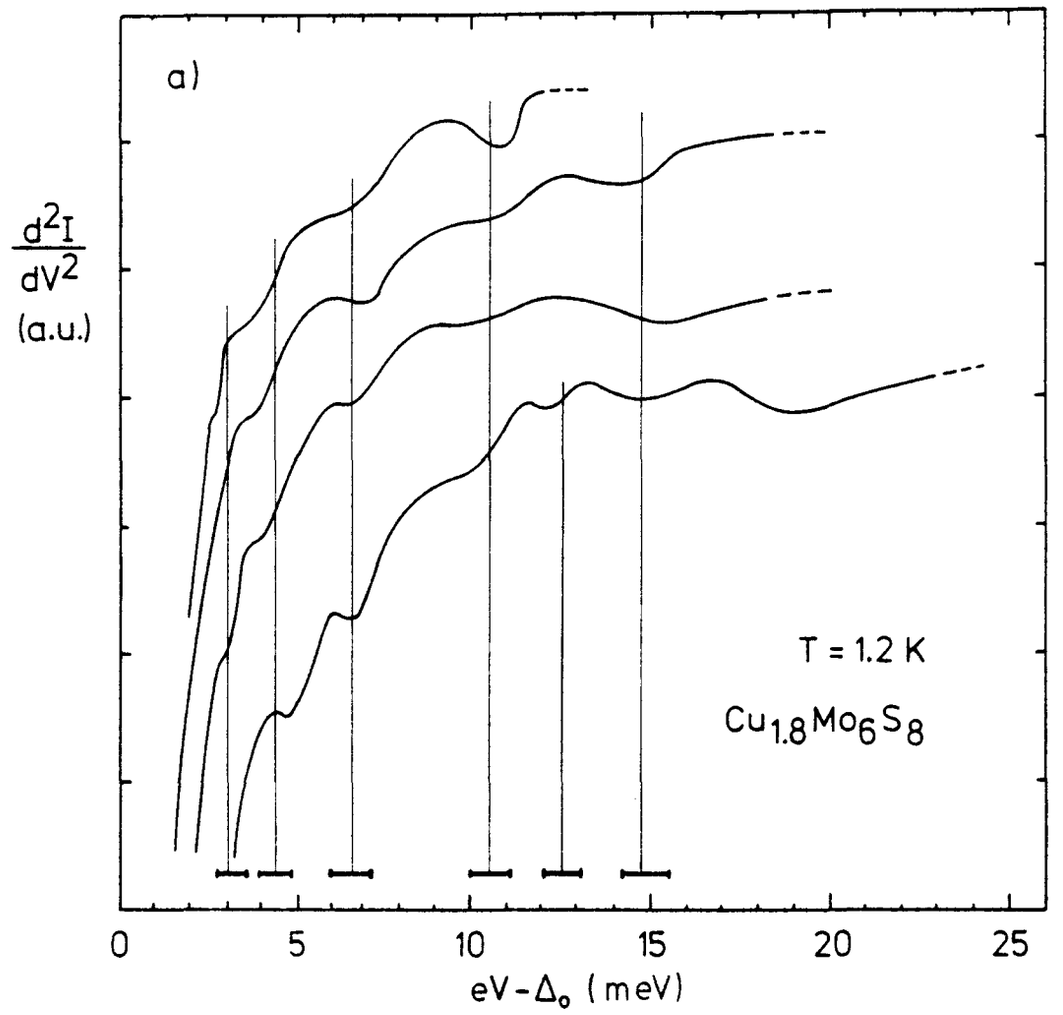
a)
$\frac{d^2I}{dV^2}$ (a.u.)
T = 1.2 K
$Cu_{1.8}Mo_6S_8$
0
5
10
15
20
25
eV - Δ_o (meV)

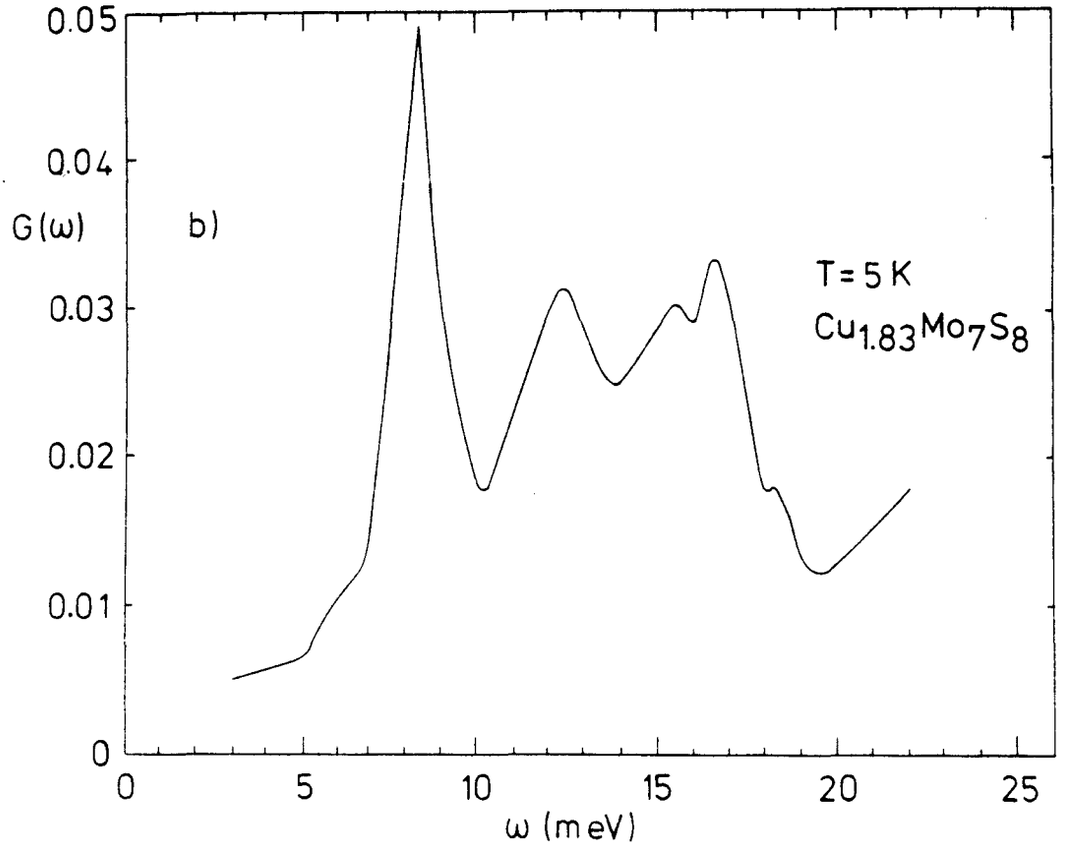
b)
G(ω)
T = 5 K
$Cu_{1.83}Mo_7S_8$
0.05
0.04
0.03
0.02
0.01
0
0
5
10
15
20
25
ω (meV)

Fig. 12

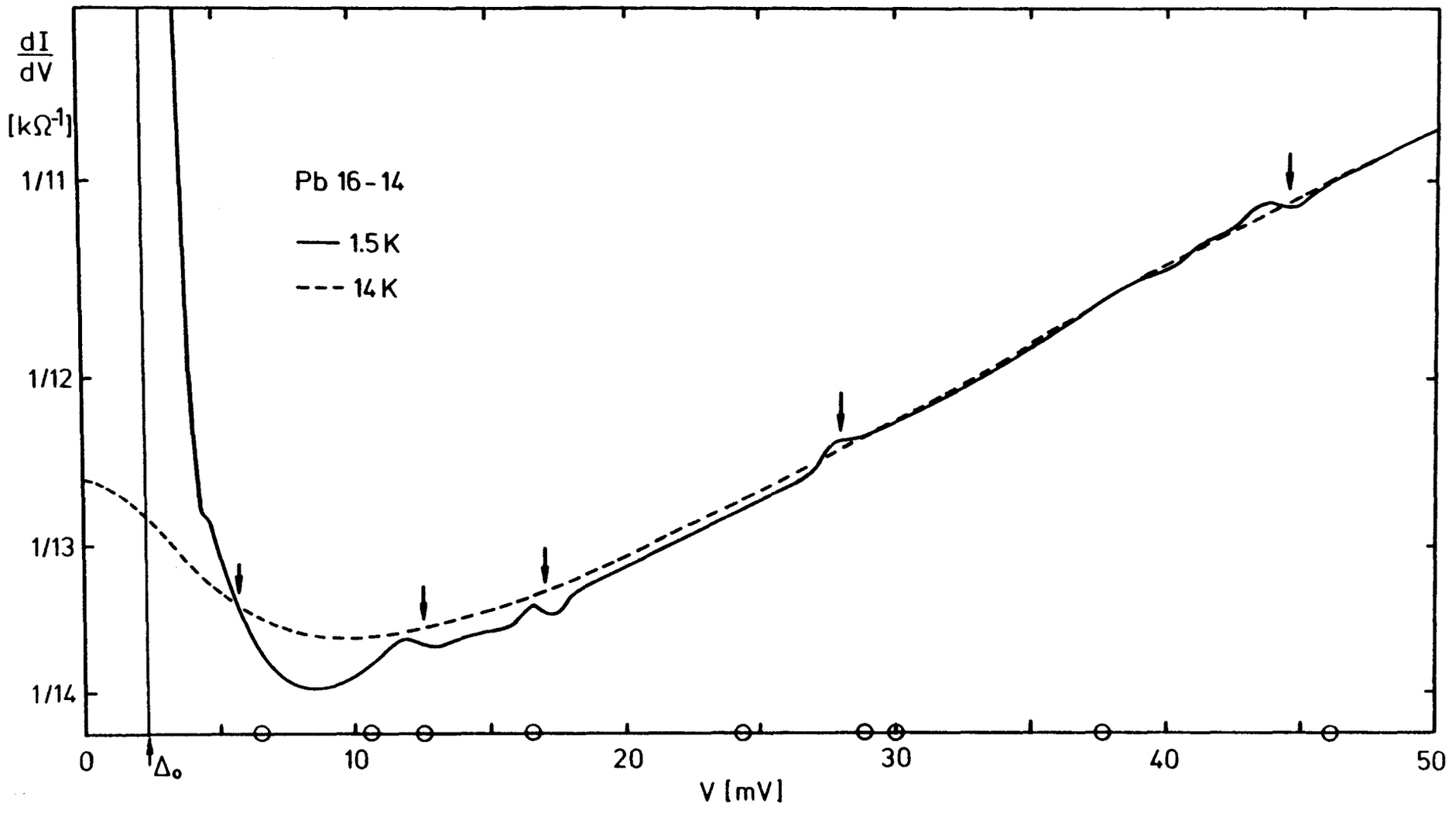

Fig. 13